

ÉCOLE POLYTECHNIQUE FÉDÉRALE DE LAUSANNE

MASTER THESIS

**Conceptual design of a bio-inspired
jumping-assisted takeoff mechanism for a
fixed-wing drone**

Author:

Tristan BONATO - 247066

Professor:

Prof. Dario FLOREANO

Supervisors:

Dr. Hoang-Vu PHAN

Mr. Won Dong SHIN

Expert:

Prof. Alessandro GIUSTI

January 21, 2022





Laboratory of Intelligent Systems

MASTER PROJECT

Title: Conceptual design of a bio-inspired jumping-assisted takeoff mechanism for a fixed-wing drone

Student(s): Tristan Bonato (Robotics)

Professor: Dario Floreano

Assistant 1: Hoang Vu Phan

Assistant 2: Won Dong Shin

Project description:

Most recent fixed-wing drones require runways or external launchers such as catapult, hand, etc. to enter into the air. These takeoff approaches limit the drones to be deployed in various complex environments as they also require an open space to land safely. Otherwise, birds in nature can perform self-takeoff and landing in various terrains by a combination of their wings and legs. To prepare for a takeoff, a bird lifts its wings up and flexes its legs for storing energy. By forcefully flapping the wings downward and pushing the feet to the ground simultaneously, the bird can start its flight journey. Previous studies indicated that jumping legs produce a takeoff thrust more than two times the body weight of a pigeon (Heppner and Anderson, J. Exp. Biol., 114, 285–288, 1985) and contribute to more than 90% of the initial takeoff velocity (Provini et al., J. Exp. Biol., 215, 4115–4124, 2012). This therefore allows some birds to take off vertically.

The takeoff mechanism of birds is thus a source of inspiration to build a robotic replica to extend the range of applications of the drones. This project will focus on design and prototype of a simple and lightweight (yet effective) bird-inspired jumping-assisted takeoff mechanism for a centimeter-scale fixed-wing drone. The student is recommended to start the project by the following steps: (1) review of takeoff mechanism of birds and state-of-the-art multimodal locomotion drones, (2) conceptual design of the jumping-assisted takeoff mechanism, (3) jumping takeoff kinematic and dynamic analyses, (4) fabrication of a prototype, and (5) experimental tests of the jumping takeoff.

Through this project, the student will gain knowledge and experience on how to transfer from biological mechanisms to their robotic counterparts. Results of the study are also potential for a publication.

Remarks:

You should present a research plan (Gantt chart) to your first assistant before the end of the second week of the project. An intermediate presentation of your project, containing 10 minutes of presentation and 10 minutes of discussion, will be held on November 11, 2021. The goal of this presentation is to briefly summarize the work done so far and discuss a precise plan for the remaining time of the project. Your final report should start by the original project description (this page) followed by a one page summary of your work. This summary (single sided A4), should contain the date, laboratory name, project title and type (semester project or master project) followed by the description of the project and 1 or 2 representative figures. In the report, importance will be given to the description of the experiments and to the obtained results. A preliminary version of your report should be given to your first assistant at the latest 10 days before the final hand-in deadline. Please make sure you comply with the regulations of your program when giving your final report before noon January 21, 2022. A 30 minute project defense, including 10 minutes for discussion, will take place between February 7 and February 18, 2022. You will be graded based on your results, report, final defense, and working style. All documents, including the report (source and pdf), summary page and presentations along with the source of your programs should be handed-in as a single compressed file on the day of the final defense at the latest.

Responsible professor:

Responsible assistant:

Signature:

Dario Floreano

Signature:

Hoang Vu Phan

Lausanne, 24 September 2021

Contents

| | | |
|----------|--------------------------------------|-----------|
| 1 | Introduction | 1 |
| 2 | State-of-the-art | 2 |
| 2.1 | Jumping robots | 2 |
| 2.2 | Jumping and gliding robots | 3 |
| 2.3 | Jumping and flying robots | 4 |
| 3 | Prototype working principle | 5 |
| 4 | Simulations | 7 |
| 4.1 | First assumptions | 7 |
| 4.2 | Spring simulation | 9 |
| 4.2.1 | Spring model | 10 |
| 4.2.2 | Spring's result | 11 |
| 4.3 | Balistics | 12 |
| 4.3.1 | Mathematic model | 12 |
| 4.3.2 | Ballistics results | 14 |
| 5 | Design of the robot | 17 |
| 5.1 | Propulsion | 17 |
| 5.2 | Compressive mechanism | 17 |
| 5.2.1 | Freewheel | 17 |
| 5.2.2 | Gear box | 18 |
| 5.2.3 | Decoupling mechanism | 19 |
| 5.3 | Spring | 20 |
| 5.3.1 | Pivot | 21 |
| 5.3.2 | End of beam | 21 |
| 5.3.3 | String Path | 21 |
| 5.4 | Wing-tail | 22 |
| 5.5 | Components | 24 |
| 6 | Prototype | 25 |
| 6.1 | Spring test | 25 |
| 6.2 | Gear box | 26 |
| 6.3 | Final prototype | 26 |
| 7 | Experimental test | 29 |
| 8 | Results | 30 |
| 8.1 | Test 1 : without propeller | 30 |

| | | |
|-----------|-----------------------------------|-----------|
| 8.2 | Test 2 : with propeller | 32 |
| 9 | Discussion | 32 |
| 10 | Conclusion | 33 |
| 11 | Acknowledgments | 34 |

List of Figures

| | | |
|----|--|----|
| 1 | Images of jumping robots | 3 |
| 2 | Images of jumpglider | 4 |
| 3 | Images of jump and fly robot | 4 |
| 4 | Flow diagram | 5 |
| 5 | Schema of the drone with the jumping mechanism | 6 |
| 6 | First model on Solidworks | 7 |
| 7 | Flow simulation | 8 |
| 8 | Schema of the spring | 10 |
| 9 | Plot of spring from Matlab | 12 |
| 10 | Mathematical model | 13 |
| 11 | Plot of ballistic results | 15 |
| 13 | Plot of ballistic results for 35° | 15 |
| 12 | Plot of ballistic results without rotation | 16 |
| 14 | Image of motor | 17 |
| 15 | Illustration of the gearbox | 18 |
| 16 | Illustration in detail of the gearbox | 19 |
| 17 | Illustration of the decoupling mechanism | 20 |
| 18 | Illustration of the drone when springs are compressed | 21 |
| 19 | Illustration of the path string | 22 |
| 20 | Images of the data of the airfoil | 23 |
| 21 | Images of the connection of the tail | 24 |
| 22 | Image of the prototype 1 | 25 |
| 23 | Image of the prototype 2 | 26 |
| 24 | Images of Gears detail | 28 |
| 25 | Images of final prototype without propeller | 29 |
| 26 | Images of final prototype full | 29 |
| 27 | Plot of the position and speed on different configurations | 30 |
| 28 | Plot of the characteristics of the jump | 31 |
| 29 | Images of the jump in OptiTrack | 32 |

1 Introduction

A drone that can perform a high speed and long-endurance flight, self-landing and self-takeoff in confined spaces, and high manoeuvrability, is useful for many applications. However, it is challenging to have all of these characteristics in a single platform. Drones are categorized in two types: fixed-wing and rotary-wing. The rotary-wing drone has advantages of agility, manoeuvrability and simple take-off by direct control of lift, but has relatively short flight endurance and low speed. On the other hand, the fixed-wing vehicle has advantages of high speed and long-endurance flight but requires sophisticated take-off strategies. It is because the fixed-wing vehicle requires a certain forward speed to take-off, and the lift generation is a function of forward speed. To reach the required speed for take-off, the drone can be thrown by hand, have wheels to drive on the road like a plane, or use an external mechanism to propel. However, these methods limit the drone to be deployed in complex environments, where human supervision and clear runway are unavailable. As a result, the applications of fixed-wing drones are limited.

Unlike the fixed-wing drones, flying animals do not need external mechanisms or a runway for take-off. Locust is an example: it uses legs to jump to have enough speed and height for take-off [1]. Many bio-inspired jumping robots have been developed, such as Mowgli: A Bipedal Jumping and Landing Robot [2], A Bio-Inspired Hopping Kangaroo Robot [3], and many others [4]. Nevertheless, there are not many robots that can perform both jumping and flying although some can jump and glide like [5], [6] or [7]. To the best of our knowledge, Passerine is the only drone that demonstrated the concept of jumping-assisted take-off [8]. However, no technical data have been shown.

Jumping to take off has many advantages. The primary point is to land and take off itself without human interference. Thus, the drone can take off even if the access is restricted, like on the roof of a building or behind a barrier. Furthermore, contrary to a wheeled drone, it can take off even if the place in front of the drone is minor or in bad condition. Finally add that the take-off process is fast. With the jumping legs, the drone can also acquire quick take-off process.

This project aims to provide an ability to do an in-place take-off to a fixed-wing vehicle by adding an on-board jumping mechanism. Weight is a critical fact on the flying performance. To avoid adding excessive weight from the jumping mechanism, a single actuator is used to actuate the propeller for flying mode and the jumping mechanism by storing energy in an elastic component.

In this report, we present the following topics. First, we review the current state of the jumping robots and gliders. Second, we design a simple jumping-assisted takeoff mechanism and explain the working principles of the mechanism. We then establish a model of the drone and simulate the kinetics and dynamics of the ballistic jump. Thereafter, we fabricate a fixed-

wing robot prototype. Finally, we set up and perform experiments on the jumping takeoff performances of the robot.

2 State-of-the-art

To date, there are many studies on the jumping robots. However, few publications present the jump as a means of propulsion for gliding. When it comes to jumping and flying, research is almost non-existent. Below, we expose the current state of the art for these three categories.

2.1 Jumping robots

Over the past decades, researchers have been particularly interested in jumping robots, leading to developing a wide variety of jumping mechanisms. However, most of these robots do not match our project's prerequisites. Indeed, to help the takeoff, the robot must jump to increase its forward speed to contribute to the wing's lift. That means all the robots that have a vertical jump are not relevant for us, like JumpRoACH [9], the Jumping-Crawling Robot [10], and the vertical jumping robot from Duncan et al. [11]. Furthermore, to minimize extra components, the actuators should not be used only to propel, like the friendly and complex frog robot from Niiyama et al. [2]. Finally, the robot needs to perform a smooth jump to reduce the drone's body rotation, unlike this kick and bounce mobile robot from Takashi Tsuda, et al. [12].

Three remarkable articles meet the constraints for flight:

- The first article presents a robot based on a kangaroo [3]. To propel the robot, it uses two feet represented by a half-circle as shown in Fig. 1.A. A torsion spring located on the hip allows to store energy. Finally, a tail is used to control the body rotation.
- The second article is inspired by the locust to create a robot [1]. It imitates the "muscular" and "bone" structure from the locust to produce a lightweight and reasonably efficient jumping drone as in Fig. 1.B.

Like the locust, the robot has two legs. Each leg is composed of a tibia, and a femur, replaced by two rigid bars. The muscle is replaced by a torsional spring compressed by a small motor. The results of this robot are impressive for the height of the jump and its lightweight. The main drawback is the chaotic body rotation after jumping.

- The last article shows a 7g miniature jumping robot [13]. It is a miniature jumping robot with two legs composed of a tibia and femur as in Fig. 1.C. The robot has an impressive jumping performance (1.4m for 7g robot). Furthermore, the article gives good advice to control the takeoff without slipping. The main drawback is the complexity of the mechanism.

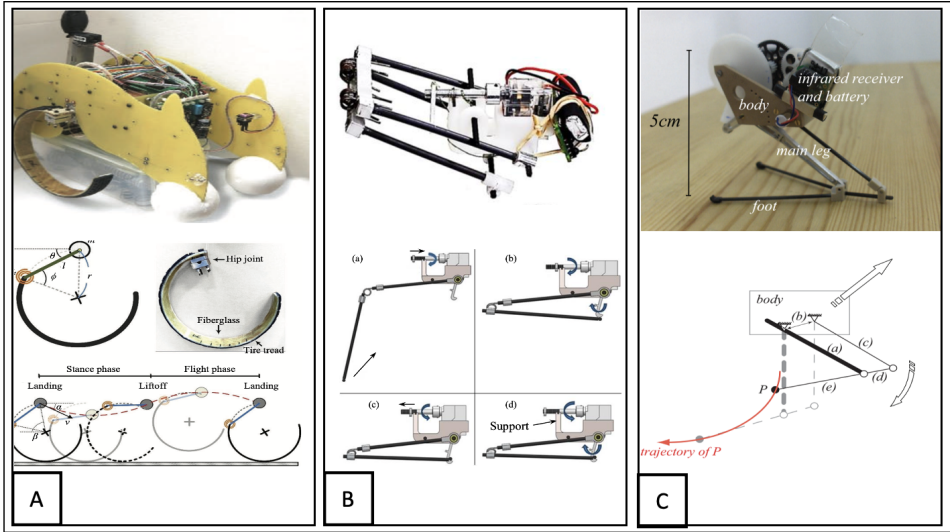


Figure 1: *Images of the three jumping robots and the detail of their jumping mechanisms.* (A) the Kangaroo bio-inspired robot. (B) the Locust robot. (C) the 7g miniature robot.

2.2 Jumping and gliding robots

The number of articles for the jumping-gliding robots is drastically smaller. We also do not intend to present robots that jump vertically, even if it glides after, like the MultiMo-Bat [14], because of the difficulty to begin to fly after a mainly vertical trajectory. We expose here three relevant articles for our goal.

- The Fig. 2.A shows the drone presented by Avishai Beck et al. [15] presents a wing-spreading locust-inspired jumpglider. The drone uses the same mechanism presented by Zaitsev et al. [1] for jumping. To allow the drone to glide and stabilize, Avishai Beck et al. added retractable wings.
- An exciting article is the one about the EPFL jumpglider [7]. The Fig. 2.B reveals a hybrid jumping and gliding robot with rigid or folding wings. The folding wing decreases drag while correcting the body rotation of the robot during takeoff. It is a lightweight and streamlined design.
- The robot from Desbiens et al. [6], shown in Fig. 2.C, is designed for efficient repeated jump and glide. It propels the drone with two rigid carbon beams. One high torque motor compresses the beams and clips a magnetic system to stay compressed. Then when released, the drone jumps. We find a particular interest in this one. The propelling mechanism is lightweight and adjustable for a fixed-wing drone.

The main drawback of these jumpgliders is that the system is not designed to fly but only to glide. The motor with high torque and low speed can not be used to create thrust, and its position is not appropriate to fly. All these structures can not welcome the component to fly.

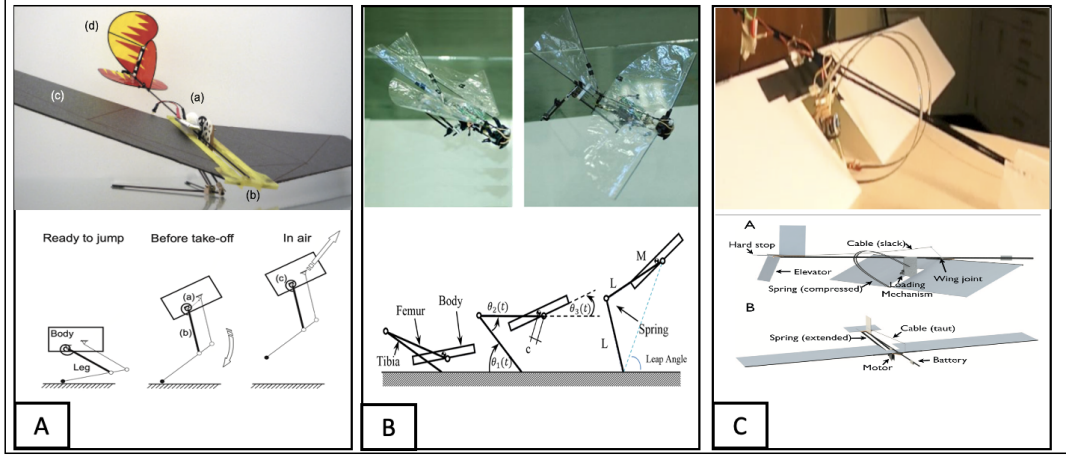


Figure 2: *Images of the three jumpgliders and the detail of their systems. (A) the locust-inspired jumpglider. (B) the EPFL jumpglider. (C) the efficient repeated jumping and gliding robot.*

2.3 Jumping and flying robots

The studies on jumpflyer are even poorer than on jumpglider. Indeed, we found only one fixed-wing drone developed by Passerine [8] that demonstrates the concept of jumping-assisted takeoff. They build a drone with robust legs that make the drone jump as shown in Fig. 3. Although the drone demonstrated a flight with the jumping mechanism, it still faces challenges in jumping stability and can not perform jumping takeoff.



Figure 3: *Images of the robot from Passerine and a detail of its jumps.*

These works give us ideas to create a drone that can jump and fly with a lightweight onboard mechanism. In this work, we adapt the jumping mechanism from Alexis Lussiens et al. [5]. However, we develop the winching system that enables the drone to activate the flight mode after jumping.

3 Prototype working principle

This project aims to create a jumping mechanism assimilated to a fixed-wing drone. Flying performance is critically affected by the weight of the system. Therefore, adding a jumping mechanism to a fixed-wing vehicle can lower the flying performance. In the worst case, the vehicle may not be able to fly. Our strategy to avoid lowering the flying performance is to use parts of aerial locomotion for jumping mechanism to avoid adding extra weights. To be more specific, we use the electric motor, which is used for the propeller, to store elastic energy in the jumping mechanism.

The type of UAV that we use is called a twin-boom. It has one wing with a fuselage and two bars connected to the tail. We aim to use the two bars as source of elastic energy by selecting carbon fiber beams as the material. Bending the two carbon beams stores energy to give the robot enough speed and height for the take-off. The carbon has many advantages. It has a high energy density, it has a high ratio rigid/weight, and it has a high yield stress that permit the material to deform and go back without deformation. This idea has been implemented in jumpglider drones [5, 6]. Although these drones were able to produce enough speed from the stored energy to take-off, it could not continue flying because they did not have the appropriate motor for thrust. We see that the main drawback of the drones is the usage of the motor just for the compression. Indeed, the motor used a high torque that can not be reused to fly because of its low turning speed. We propose to reuse the motor installed for the thrust to store energy in the beams. Since the carbon fiber beams work as torsional springs, we will call the beams as springs until the end of the report.

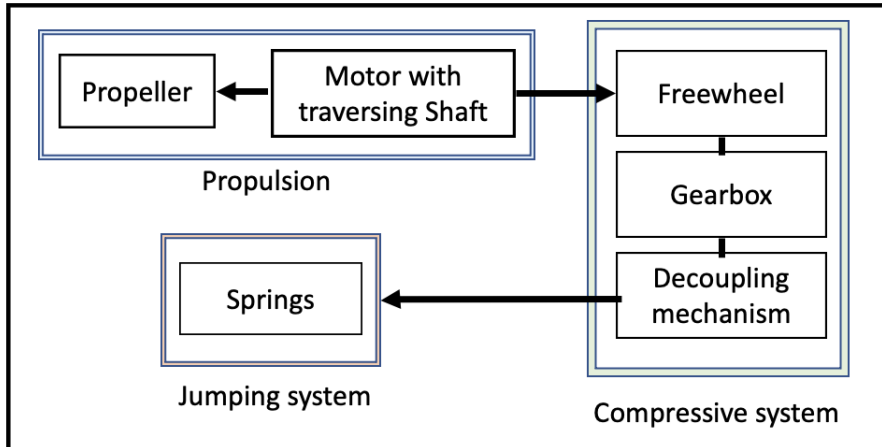


Figure 4: A diagram that explains the connection between each subsystem. The motor is connected on one side to the propeller and on the other side to the compression system (freewheel, gearbox, and decoupling mechanism). Then the compression system is connected to the jumping system (the springs).

Before explaining the principle of the springs, we detail the compressive mechanism here. Fig. 4 shows how the subsystem are connected together. As we mentioned in the previous paragraph, we aim to use the motor already presented on the drone. Therefore, We use a motor with a transversal shaft to exploit the available space. It means that the shaft is passing through the engine. One side is used to create thrust by connecting to a propeller, and the other side is connected to the compressive mechanism.

To split the two functions of the motor, we use a freewheel. The freewheel is connected to the side of the compressive mechanism. It allows the motor to engage with the compressive mechanism when rotation in one direction and disengage when the motor rotates in the reverse direction (to power the propeller). A gear box is used to increase the torque from the motor to drive the compressive mechanism.

The last important part is the release process. We want that the springs are released at a precise moment and without adding extra control components like servos or sensors. Therefore, we design a half-teeth gear that lets the springs release right after the gear teeth disengage.

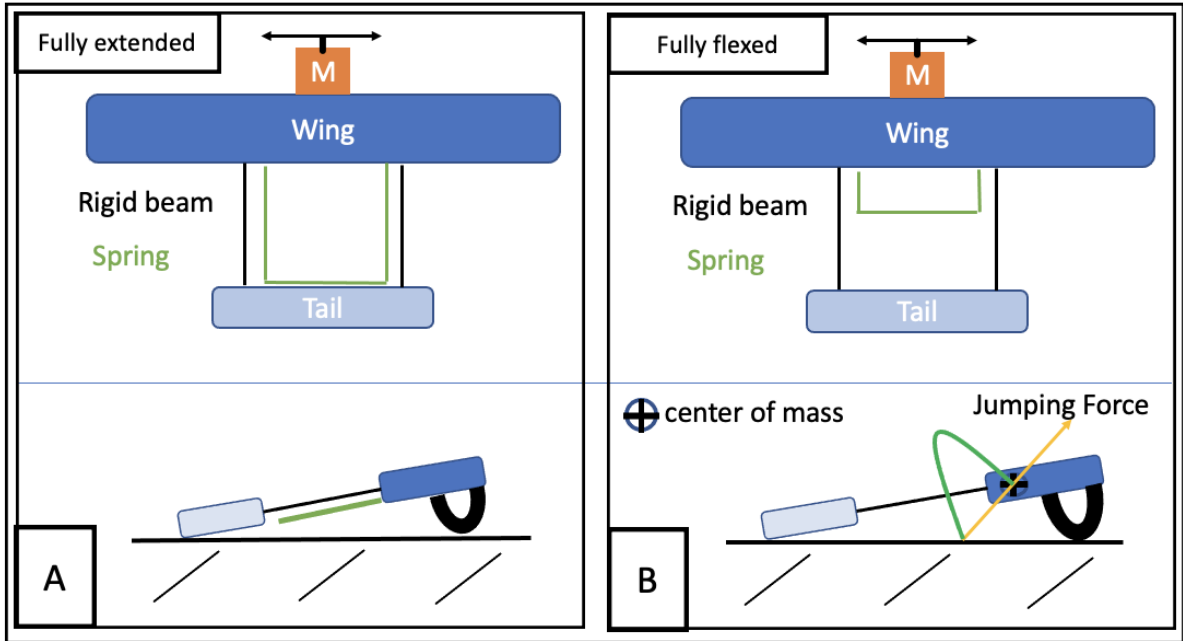


Figure 5: *Schema of the jumping mechanism in two different configurations: (A) fully extended stage, and (B) fully flexed stage. The schemes on the top show the top-view of the drone and the schemes on the bottom show the drone from the side-view.*

Now let's focus on the springs. To accumulate the energy needed for flight, the spring must compress. In the Fig. 5, we have an illustration of the drone in two different stages: fully extended and fully flexed. One end of the spring is connected to a pivot near the centre of mass. The other extremity is aligned to the tail when not compressed (Fig. 5.A) and touching the ground when compressed (Fig. 5.B). A string is connected to the end of the spring to compress. It passes through the axis of rotation of the pivot to minimize torque on the drone.

4 Simulations

To build the drone, we first performed theoretical calculations and simulations. We built a preliminary model on Solidworks and estimated essential information such as size, minimum flying speed, inertia, and weight based on the required components of the drone. This is the starting point of the design and to have a general idea of what we can achieve with the geometry. Then, we made a model using MATLAB to find the appropriate properties of the spring. We want to understand how the shape of the spring affect its characteristics (energy, stress,...). Finally, we built a MATLAB model to study the plane's behaviours after take-off. We aim to study the ballistic jump of the drone and estimate its potential. In this simulation, we made a particular point to have minimum body rotation, enough height, and sufficient speed to fly.

4.1 First assumptions

A dynamics model of the take-off requires initial values of mass, inertia, dimension, and center of mass location of each component such as the carbon spring, fuselage, and the wings. To obtain these initial values, we designed the prototype on Solidworks. The Fig. 6 shows the model. In addition, aerodynamics properties such as the minimum speed for take-off and the coefficient of lift and drag of the wing were obtained through Solidworks.

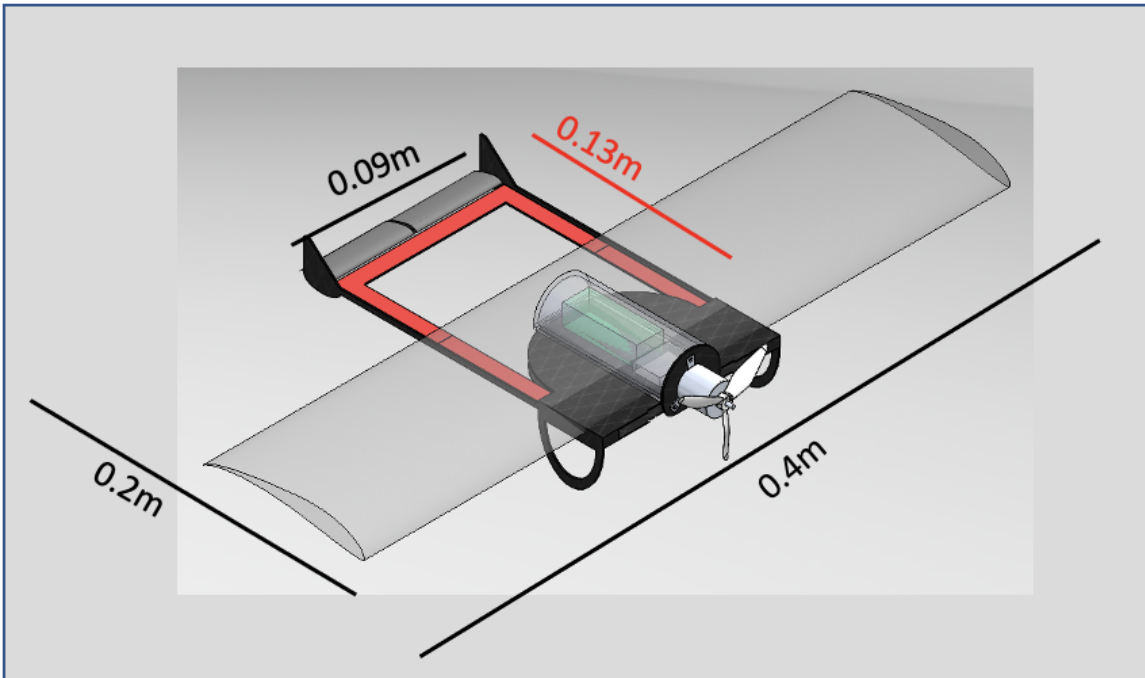


Figure 6: *This image shows the first model made on Solidworks. It gives the size of the drone and the shape. Furthermore, it gives an initial idea of the place of the springs (in red).*

Physical properties Solidworks automatically give the physical values after having the model and applying the materials.

Aerodynamics properties In this section we want to find the minimum speed to fly. Furthermore, we want to include aerodynamic forces in a dynamics simulation. Thus, we need to know the lift and drag coefficients of the wings as equations (1) and (2).

$$L = 1/2\rho V^2 S_{ref} C_L \quad (1)$$

$$D = 1/2\rho V^2 S_{ref} C_D \quad (2)$$

where L denotes the lift force, V is the velocity of aircraft expressed in m/s, ρ is the air density, S_{ref} is the wing area in square metres, C_L and C_D are the coefficients of lift and drag, respectively.

Solidworks provides a simulation tool called Flow Simulation that calculates the lift and drag with a given aircraft velocity and angle of attack. With its help, we obtained the minimum speed (6 m/s with wing's angle of attack = 10°) required to generate 1.5 N of lift for take-off. The Fig. 7 shows the vector of pressure from the simulation at 6 m/s and 10°.

Using this tool and the previous equations, we obtained the lift and drag coefficients profile of our prototype.

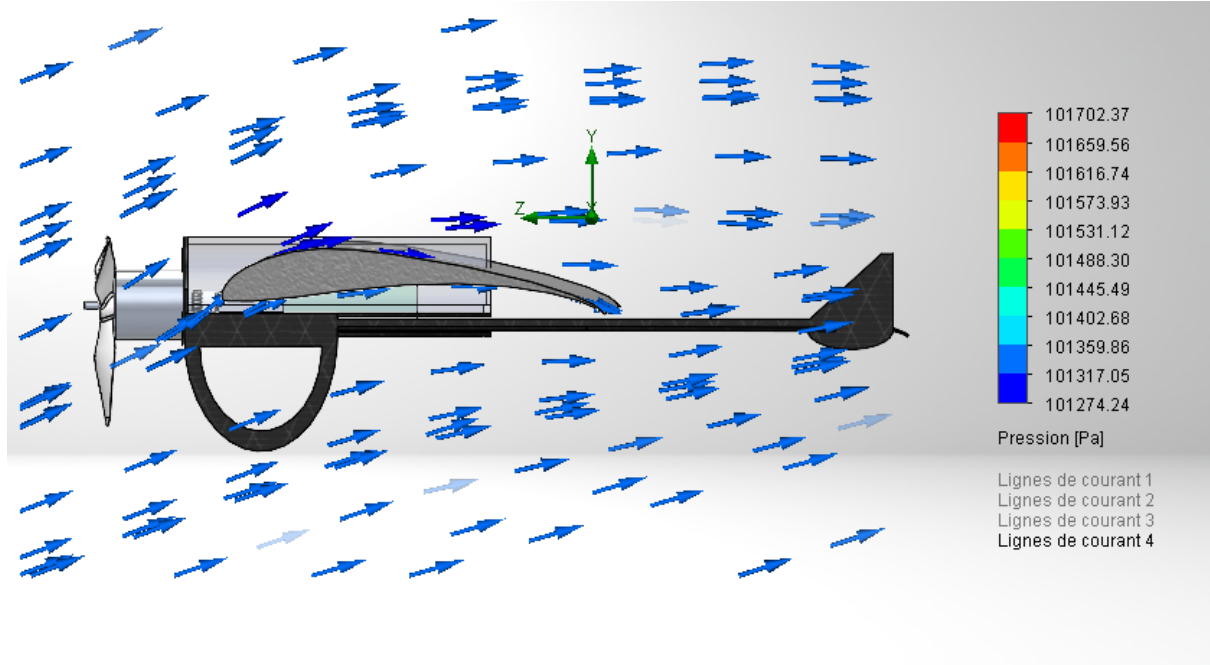


Figure 7: This image shows the vector of pressure around the wing in Solidworks during flow simulation. The speed is set up a 6 m/s with an angle of 10°. The vector of pressure are lower below the wing and higher above it.

Table 1: constants

| Kind of | Definition | Values |
|--------------|------------|---------------------------|
| Physical | Mass | 0.15 Kg |
| | Inertia | 0.00016 Kg/m ² |
| Aerodynamics | Min. speed | 6m/s |
| | Angle | 10° |
| | Lift | 1.5N |
| | Drag | 0.3N |
| | Cl | 1.2851 |
| | Cd | 0.04798 |

4.2 Spring simulation

This section exposes all the main points to simulate the springs and their characteristics. Before explaining the model and the result, we talk about preliminary information.

The springs are designed in a function of the energy they can absorb during compression. Therefore, we calculate the energy needed to obtain the required take-off velocity and height. The velocity is primary to have enough lift from the wing to fly. From the previous section, we found that 6 m/s is enough to make the drone fly. Furthermore, the height of 0.5 meters is to avoid the obstacle and increase time in the air. The time in the air is crucial to let the propeller have an effect. From the energy equations (3), (4) and (5), we can find the potential energy needed for the springs to propel the drone, where m is the mass, v is the velocity, g is the gravitational constant and h is the height.

$$E_{cin} = \frac{1}{2}mv^2 \quad (3)$$

$$E_{pot} = \frac{1}{2}mgh \quad (4)$$

$$E_{Spring} = E_{pot}E_{cin} \quad (5)$$

The required potential energy in the springs is 3.5 Joule.

4.2.1 Spring model

The goal of this section is to find a proper shape of a carbon fibre beam with its energy (to achieve expected jumping performance from the previous section) and its maximum shear stress (to prevent damage while compressing). We purchased carbon fibres with a cross section of 3 mm x 0.6 mm from Swiss composite (<https://shop.swiss-composite.ch/>). The carbon fibre has a tensile modulus $G = 60$ Gpa and a maximum shear stress $\sigma = 1.3$ Mpa. The energy stored into the beam is equal to equation (6) and (7), where I is the second moment of inertia, q is the deformation angle in radian, and k is the constant of rigidity of the spring.

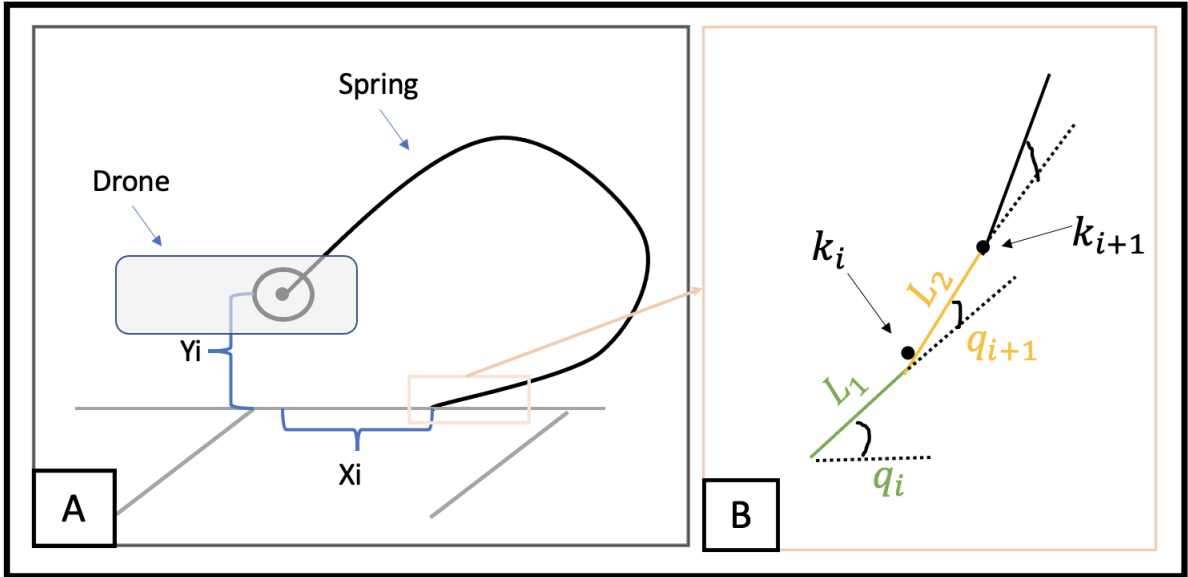


Figure 8: *Illustration of the spring (A) and its detail (B). Figure (A) shows the spring in fully flexed stage. Y_i and X_i are the coordinates of the end of the beam in function of the pivot. Figure (B) is a zoom of the end of the beam and illustrates the equation (6). It shows three sub-segments of the bar (L_i), their rigidity (k_i) and deflections (q_i).*

All the spring's equations we used work only at small deformation. It is why we divide the bar into 40 small elements, δL . The representation of the spring is shown in Fig. 8.

$$\begin{aligned} \underset{q_i}{\text{minimise}} \quad & \left(\frac{1}{2} \sum_{i=2}^{40} k_i \cdot q^2 \right) \\ \text{subject to} \quad & \text{End of bar} = (X_i, Y_i) \end{aligned} \tag{6}$$

$$\text{Bar position} \geq 0$$

$$k_i = \frac{G * I_i}{\Delta L} \tag{7}$$

To ensure that the bar is strong enough during compression, we use equation (8) to verify

that the maximum shear stress inside each small element does not exceed σ .

$$\sigma = \sqrt{\frac{q^2 * \delta L}{3 * E}} \quad (8)$$

$$\tau = -kq \quad (9)$$

$$U_s = \frac{1}{2}kq^2 \quad (10)$$

In the work of Alexis Lussier et al. [6], the results shows that the optimal jump angle for a flat surface is 52° under 1 m. Nevertheless, our point is to minimize body rotation. For this reason, we supposed that the best angle to propel the drone with our objectives (minimum body rotation and maximum tangential speed) is equal to 35° . We will test this hypothesize in the next section 4.3.

From section 4.1, the length of the spring is equal to 0.13 m, and the height at the pivot is equivalent to 0.025 m. Thus, we can define Y_i as equal to 0.025 m and X_i as equal to 0.035 m to obtain an launching angle of 35° .

4.2.2 Spring's result

The shape of the carbon beam is not disposable in infinite possibility. It depends, of course, on the manufacturer. We do not want to find various shapes and have to check multiple companies to acquire them. Hence, we choose to command the beam on Swiss composite, and we review the different sizes of the beam at disposal for our simulation. Thus, we test different beam configurations to find a beam that will not break while storing the maximum energy. Furthermore, we need to estimate the torque required to compress the springs for the design of the compressive system.

After some hand-tuning, we choose a beam of 0.6 mm of thickness and 3 mm of width. It can store 0.55 Joule and has a maximum shear stress of $8.39e+08$ N. With the help of equations (9) and (10) we find the torque needed to compress one spring (0.42 N.m).

Finally, to achieve the 3.5 Joule, we need at least 6 springs for a total torque equal to 2.5 N.m. Fig. 9 shows the plot for the chosen solution.

For the next step, we need to simplify the model. It is challenging to model 40 small beams in Matlab and evaluate the dynamics behaviours. Therefore, we simplified the model into two rigid bars connected by a torsion spring. The simplification is represented in Fig. 9, where the lines in red and green are the bars (called leg), and the red point is where the torsional spring is located. This simulation also gives the leg's size and all the angles.

We estimated the coefficient of rigidity k with the equation (10), with U is the energy inside the spring and q is the angle between the two legs.

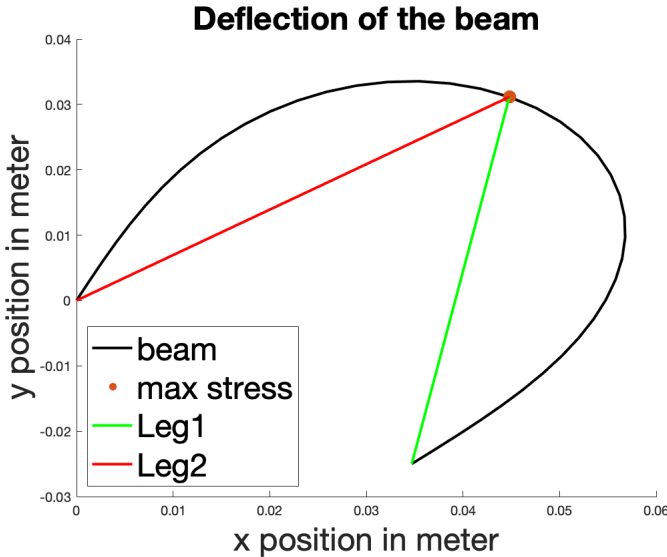


Figure 9: This figure shows the plot of the beam from Matlab. It highlights the maximum stress inside the beam, the position of the tip of the beam and the curvature. Furthermore, it shows the simplification of the beam into two rigid bars in red and green

4.3 Ballistics

This section has two main objectives. The first one is to validate the launching angle, which was hypothesized in the section 4.2 that the best launching angle is about 35° . Second objective is to test the approximation with the spring found in the previous section. We tried different initial positions in the springs simulation 4.2 to have multiple launching angles. Then, we insert the simplification into the ballistics to finally compare the data.

4.3.1 Mathematic model

Fig. 10 shows the illustration of the model. It details the model before take off (A) and a zoom of the forces close to the center of mass (B). An important detail is that the center of mass is precisely to the end of the leg 2. We hypothesized that the center of mass need to be where the jumping force is apply to decrease the body rotation.

All the code is made in MATLAB. It is challenging to input real conditions in the simulation, therefore, we simplified the simulation as follows.

- First, the friction between the ground and the end of the spring was eliminated. We assumed as a perfect pivot until the takeoff. This hypothesis is risky, but we suppose that if we add soft material like silicon at the point of contact, it will improve the friction and avoid slipping.
- In the final prototype, the connection between the spring and the body is a pivot. We made it rigidly for simplification. It means that the body and the leg 2 are colinear and rigid together.

- Finally, we do not take into account the friction of the air, aside the drag from the wing.

To improve the estimation, we added the lift and drag generated by the wing. The wing is situated at 0.01m from the centre of mass, align on one leg. The coefficient of lift and drag was found on the section 4.1.

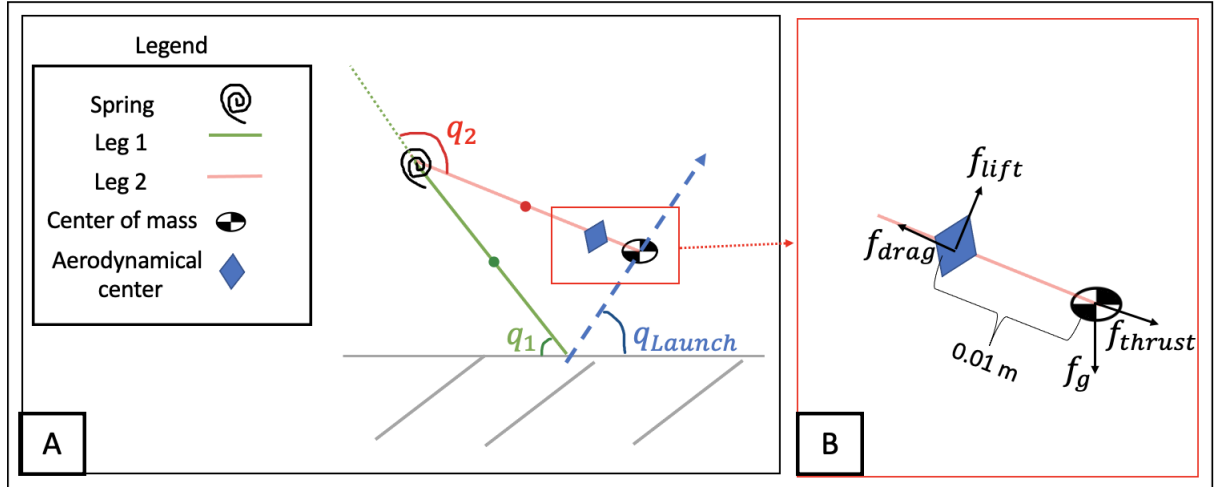


Figure 10: This figure shows the illustration of the mathematical model for the ballistics. The left one (A) shows the two legs and the spring that will propel the drone in the air. The leg 1 is touching the ground and connected to the leg 2, which is itself connected to the centre of mass of the drone. The figure on the right (B) shows a zoom around the centre of mass. It highlights the force applied on the drone in the centre of mass (force gravitational and thrust) and the aerodynamic centre from the wing (lift and drag).

For the sake of clarity, we split the problem into two subparts; the takeoff and the flight.

Take off To resolve the first part, we used the Lagrange equation (11). The leg 1 is in contact with the ground acting as a pivot.

We used the ode45 function in Matlab to resolve it. We stopped iteration when the centre of mass achieved its maximum vertical or horizontal speed.

$$\begin{aligned}
 M\ddot{q} + C\dot{q} + g &= \tau + J^T F_{\text{ext}} \\
 F_{\text{ext}} &= F_{\text{lift}} + F_{\text{drag}} \\
 \tau &= -k \begin{bmatrix} 0 \\ q_2 \end{bmatrix}
 \end{aligned} \tag{11}$$

In these equations, thrust from the propeller is not considered.

Flight When the drone leaves the ground, equations (12) are used to describe the motion. We added the thrust force generated by the propeller. The drag, gravity and thrust act on the position acceleration. But do not act on the body rotation because these forces are either on the center of mass or pointing to it. The lift of the wing and the tail act on the angular acceleration. These forces do not point to the center of mass and are not situated on it; they create body rotation.

$$\begin{aligned}
 \sum \text{Force} &= \text{mass} * \ddot{\text{pos}} \\
 \sum \text{Moment} &= \text{Inertia} * \ddot{\text{q}} \\
 \sum \text{Force} &= F_{\text{gravity}} + F_{\text{thrust}} + F_{\text{drag}} \\
 \sum \text{Moment} &= \text{DistWing} * F_{\text{LiftWing}} + \text{DistTail} * F_{\text{LiftTail}}
 \end{aligned} \tag{12}$$

4.3.2 Ballistics results

Fig. 9 shows that the spring connects to the centre of mass on one end and the ground on the other end. The foot that touches the ground has a position (Y_i, X_i) from the centre of mass. To test different launching angle, we keep $Y_i = 0.025\text{m}$ and we use ten different values of X_i in the interval $[0.02, 0.05] \text{ m}$. It gives ten launching angle between $[51;26]^\circ$.

Then, we simulated the ballistics with the simplification from the spring's simulation. Note that the spring's simulation gives the initial angles q_1 and q_2 , the lengths L_1 and L_2 and the constant of rigidity K . We also note here that we used 6 springs for the simulation from 4.2

Fig. 11 shows the tangential speed and the body rotation in function of the launching angle. We can see that the larger the launching angle is, the higher the body rotation and the tangential speed are.

Due to the body rotation, the robot may not achieve a good flight. We can minimize the body rotation by moving the center of mass forward.

We remade the simulation with a hypothesis that no body rotation occurs. This is to better understand the speed, height, and distance we can achieve and also to find a good propeller for flight. We used equation (13) to approximate the dynamic thrust from [16]

$$Thrust = 4.392399 \times 10^{-8} \cdot RPM \frac{d^{3.5}}{\sqrt{pitch}} (4.23333 \times 10^{-4} \cdot RPM \cdot pitch - V_0) \tag{13}$$

where RPM is the rotation per minute, d is the diameter of the propeller, pitch is the propeller's pitch and V_0 is the drone's speed. We used a 3-blade propeller with a diameter of 3 inches, and a pitch of 3.5. We used a motor with 1700 kv and a battery of 7.6 Volt. That gives approximately 1200 RPM.

Figs. 12 (A, B) show that the lift/drag increase the horizontal distance. Even though the drone does not reach the required initial speed to fly with only the propulsion system, Fig. 12 (C) shows that it can maintain airborne with a minimum angle of 35° launching angle with a

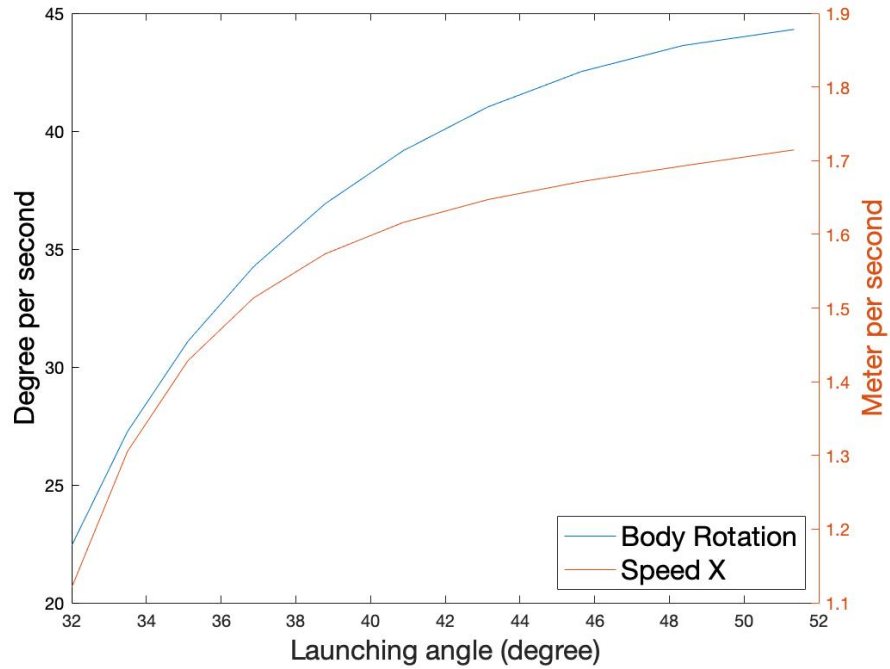


Figure 11: This plot shows the results of the ballistics simulation. It shows the tangential speed (in orange) and the body rotation (in blue) in function of the launching angle. We can see that larger the launching angle is, higher the tangential speed and the body rotation is as well.

propeller. Fig. 13 verified that, at the takeoff angle of 35° and initial speed of about 2.5 m/s, the drone trajectory becomes horizontal, which supports its flight mode. Finally, the hypothesis of the 35° launching angle seems appropriate, and we thus used this for the design of the springs and the robot.

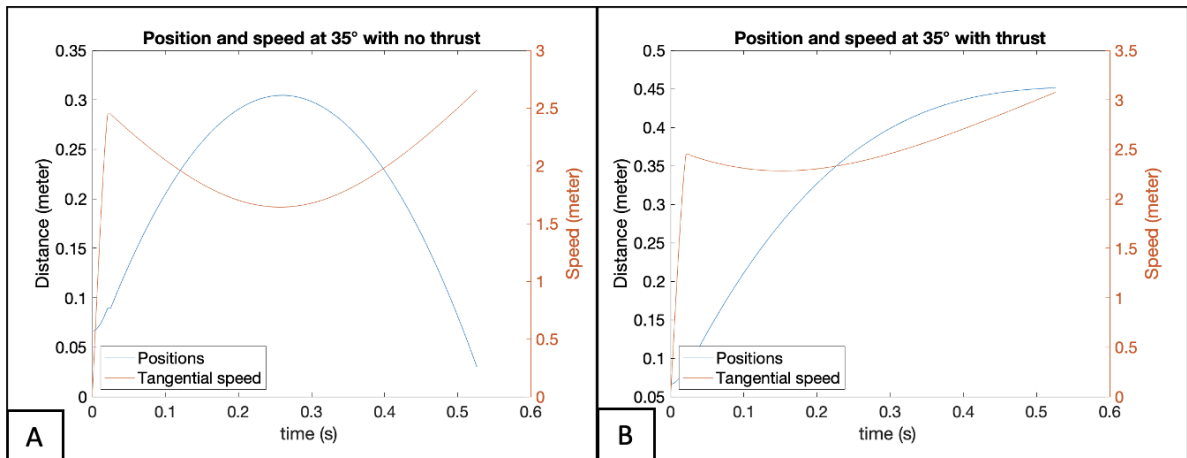


Figure 13: Trajectory and speed for the takeoff angle of 35° (A) without thrust and (B) with thrust.

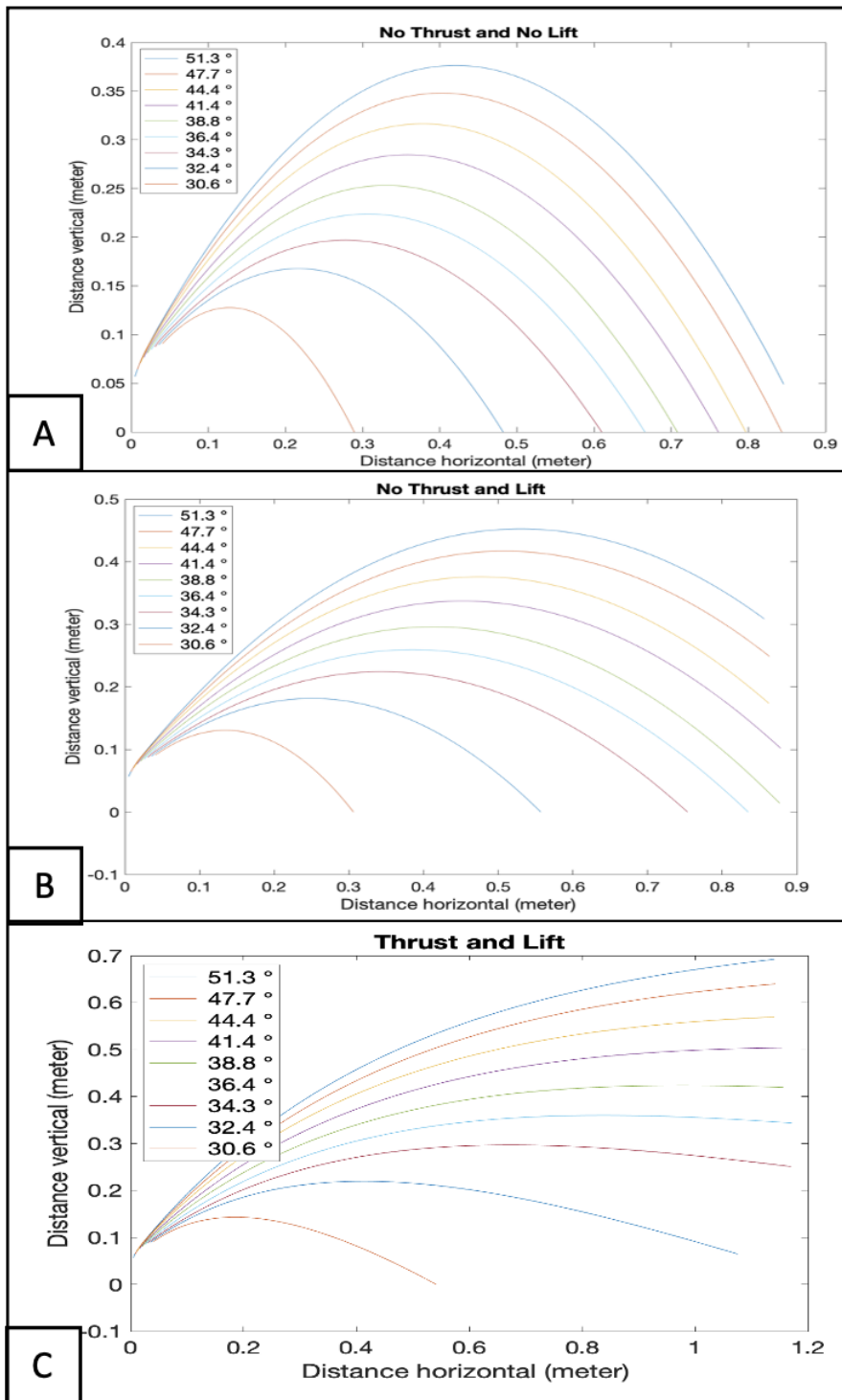


Figure 12: These plots show the result of the ballistic simulation when body rotation is stabilized. It shows trajectories in the function of the launching angle. We tested three different configurations: (A) Without thrust, and lift/drag of the wing, (B) With lift/drag but no thrust, and (C) with thrust and lift/drag.

5 Design of the robot

Fig. 4 shows a schematics that explains how all subsystems are connected. We have a motor with a transversal shaft. One side is traditionally used to create thrust by connecting to a propeller, and the other side is connected to the compressive mechanism. The compressive mechanism comprises three subsystems: the freewheel, the gearbox, and the decoupling system. The freewheel allows the motor to not turn the compressive system when we want generate thrust.. The gearbox increases the motor's torque, and the decoupling system permits releasing the spring on demand. We describe all in detail in the following sections. We also explain the shape of the wing-tail and a list of the components used.

5.1 Propulsion

To propel our drone, we use a small brushless DC motor with 1700 KV speed, as shown in Fig. 14 . By using a speed controller ESC, we can control the rotation direction of the motor to create thrust and compress the springs. The freewheel was connected to the transversal shaft of the motor. To generate thrust, we used a 3x3.5 three-blade propeller. We chose this blade to have maximum thrust but with the constraint of the 0.04 m height between the motor and the ground.

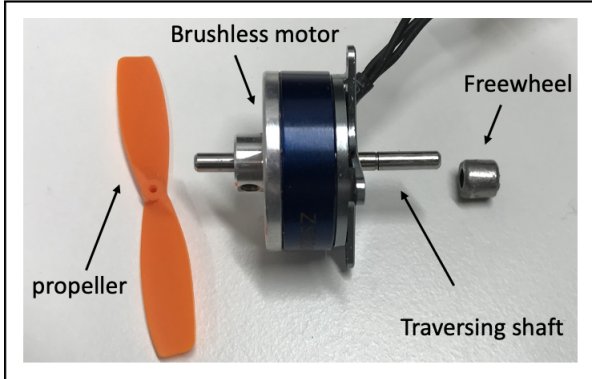


Figure 14: *The DC motor with its traversing shaft. The shaft is connected in one side by a propeller and the other side by a freewheel*

5.2 Compressive mechanism

In this section, we explain in detail the compressive mechanism and the three main subparts: the freewheel, the gearbox and the decoupling mechanism.

5.2.1 Freewheel

In the previous paragraph, we discussed that we reused the motor installed for the thrust to compress the spring. To avoid the rotation of the compressive mechanism during cruising, we

used a freewheel connected to the shaft on the compression side. Thus, when the motor turn in thrust mode (clockwise), only the propeller is driven, and when it is on the compression mode (counterclockwise), both the propeller and the compression mechanism work. Note that the propeller turns in the reverse direction that creates a little back thrust but is not strong enough to have any effect on the drone.

5.2.2 Gear box

To bind the motor to the decoupling mechanism, we used a gearbox. These gears are essential to increase the torque and decrease the speed of the motor. From the datasheet, the motor has a maximum torque of about 0.05 Nm, and the torque needed to dive the compression mechanism is 2.5 N.m as in section 4.2. Thus we need a gain more than 50 for the motor to drive the mechanism. We used a safety factor equal to 2 to counterbalance the friction of the gears made of ABS material. That implies a gain more than 100. For that reason, we used two layers of reduction gears. Fig. 15 shows the gearbox with four different points of view and Fig. 16 shows each layer of the gearbox independently. The first layer is composed of the worm gear and two spur gears (in green color). The second layer is formed by two small gear (green) and two large gears (blue). The gears with the same colours are bind together; they thus have the same rotational speed.

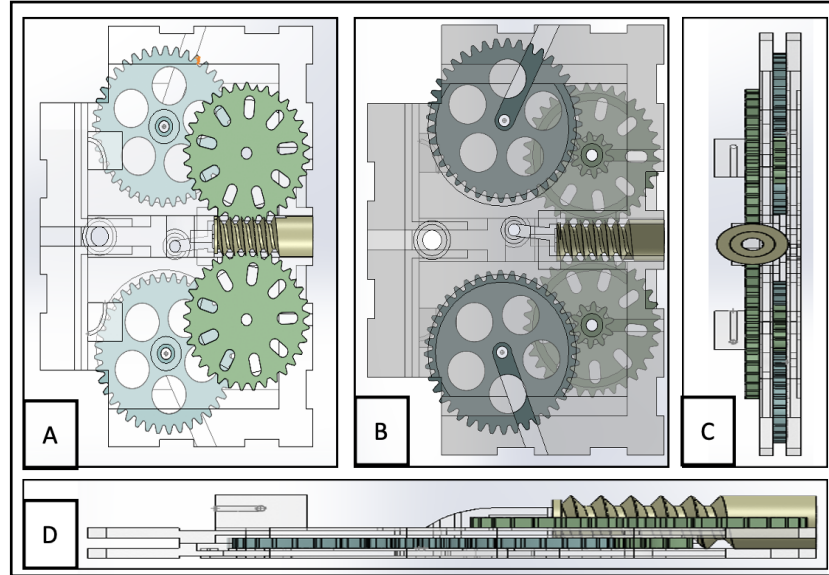


Figure 15: This image shows the gearbox configuration from Solidworks. Four different points of view are shown: (A) top view, (B) bottom view, (C) front view and (D) side view. The piece in yellow is the worm gear. It is connected to two green gears with 35 teeth. Then two inner green gears with 10 teeth are connected to two blue gears with 40 teeth. This gearbox offers a gear reduction of 140.

The worm gear offers a reduction ratio of 1:35 to increase the torque. The force is coaxial to the shaft. Thus, the shaft is not bent when the force from the springs are applied. However, the gear irreversibly prevents releasing the spring to the initial position. Therefore, we added an intelligent decoupling mechanism to release the spring when it reaches its desired position.

The total gear reduction ratio is calculated as following. The worm gear is connected to a spur gear with 35 teeth that provides a reduction of 1:35. The spur gear with inside teeth of 10 is connected to another one with 40 teeth, give a reduction of 10:40 or 1:4. Thus, the total gear reduction ratio is 1:140.

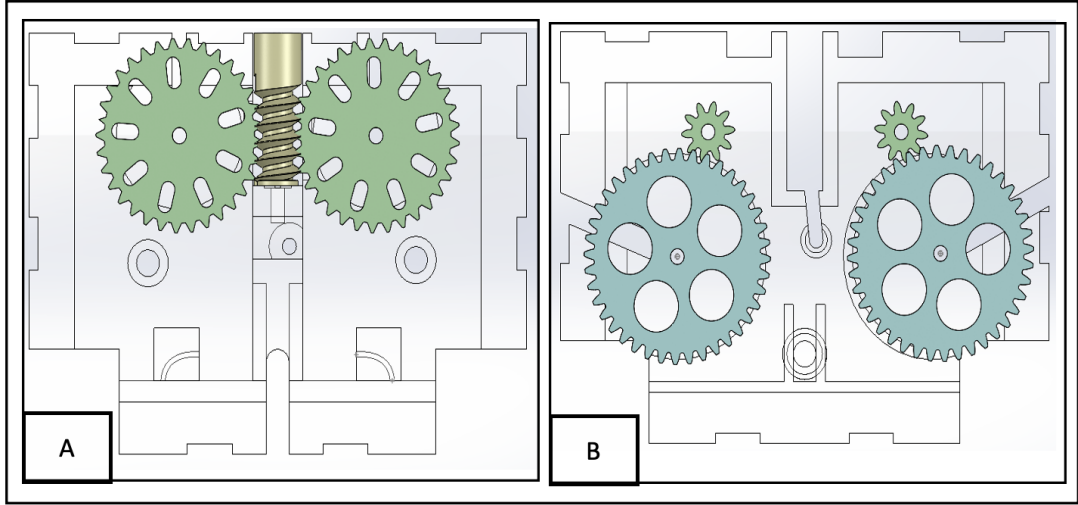


Figure 16: *Detail of each layer of the gear box for more clarity. The first layer with the worm gear (A) and the second one (B).*

5.2.3 Decoupling mechanism

Fig. 17 shows the decoupling mechanism. This mechanism can automatically release the spring without the need of any control servos or other electronic components. Furthermore, it does not require additional control system that informs the user when the spring reaches the target position.

We calculated the distance needed to compress the spring. Then, we designed a gear with a circumference that larger than the moving distance of the spring. Let us call this gear the decoupling gear (in blue) with only 3/4 teeth. The decoupling gear is fixed with the big blue gear in Fig. 16.B. Thus, it turns continuously and simultaneously with the motor (with a lower speed, of course, due to the gearbox). Then the retractor (in red) is bound to a standard gear with complete teeth around (in red also). When the teeth of the retractor are connected to the teeth of the decoupling gear, the retractor turns and the spring is compressed until it reaches the part without teeth of the decoupling gear. Then, there is no more contact between both, and the retractor is freely rotate in reverse direction to release the springs to their original position because of the compression force of the spring. Thus, the robot jumps.

To reiterate the operation, the decoupling gear will continue to turn for the subsequent compression until the teeth are engaged for the next jump.

The configuration is nearly symmetrical to avoid instability during the jump. Only one small gear (in grey) is added to correct the sense of rotation created by the worm gear. One drawback of this system is because of the geometry of the drone, the decoupling system is connected to a gear that is directly connected to the retractor gear with 30 teeth. Thus it decrease the gain by a factor $4/3$. We finally have a gain equal to 105. It is enough for our theoretical compression.

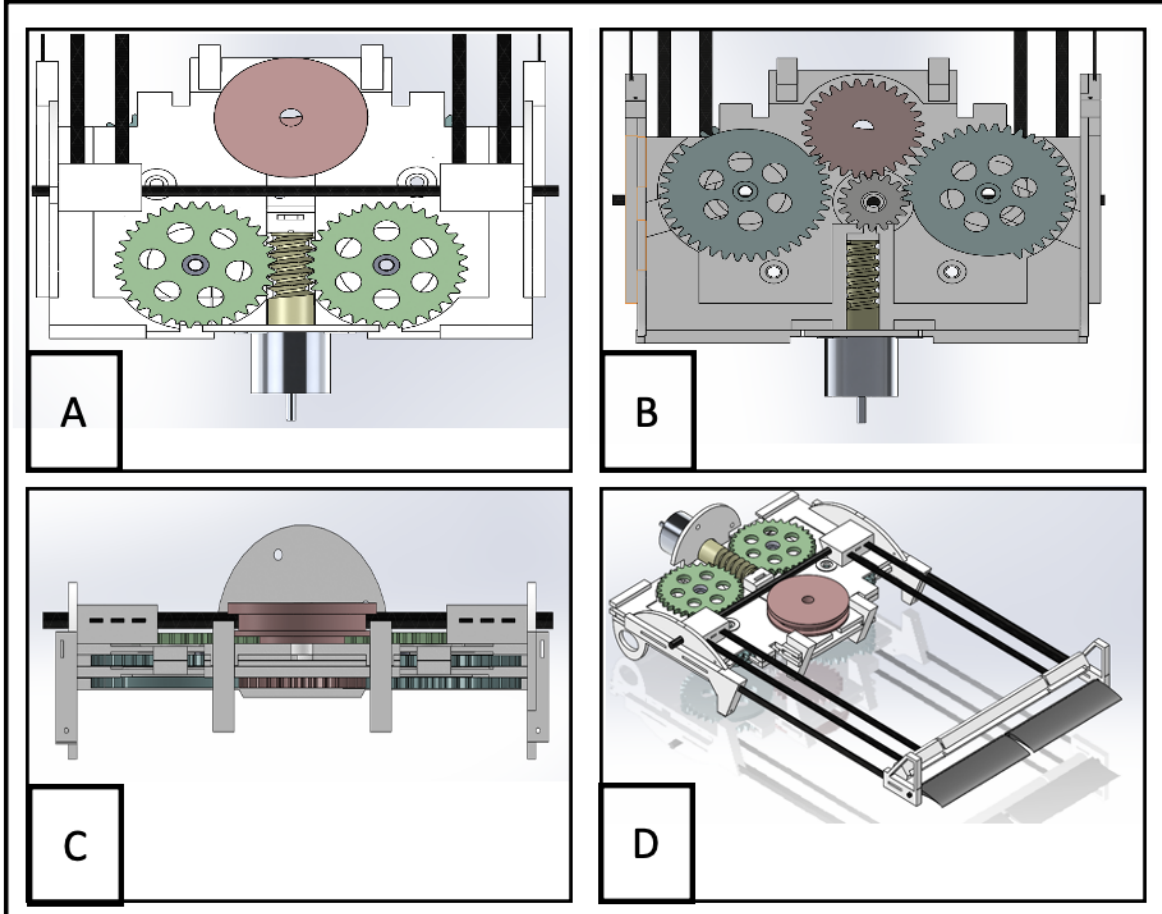


Figure 17: *The decoupling system. It has two layers; one on the top of the drone (A) and one on the bottom (B). The decoupling gear is in blue and the retractor is in red. We have four different views; the top view (A), the bottom view (B), the back view (C) and the isometric view (D).*

5.3 Spring

We used six carbon strips represented as six springs. The springs are connected to the drone by a pivot. The other sides of the beams touch the ground. The springs are compressed with the help of a string. We explain these three subparts; the pivot, beam's end, and the string path.

5.3.1 Pivot

The pivot is an essential point of our drone. It permits compressing the springs without transmitting torque into the robot. The pivot is built with two small pieces made of ABS material connected together by a carbon rod as illustrated in Fig. 18. Then the carbon rod passes through the side of the drone to be connected with it.

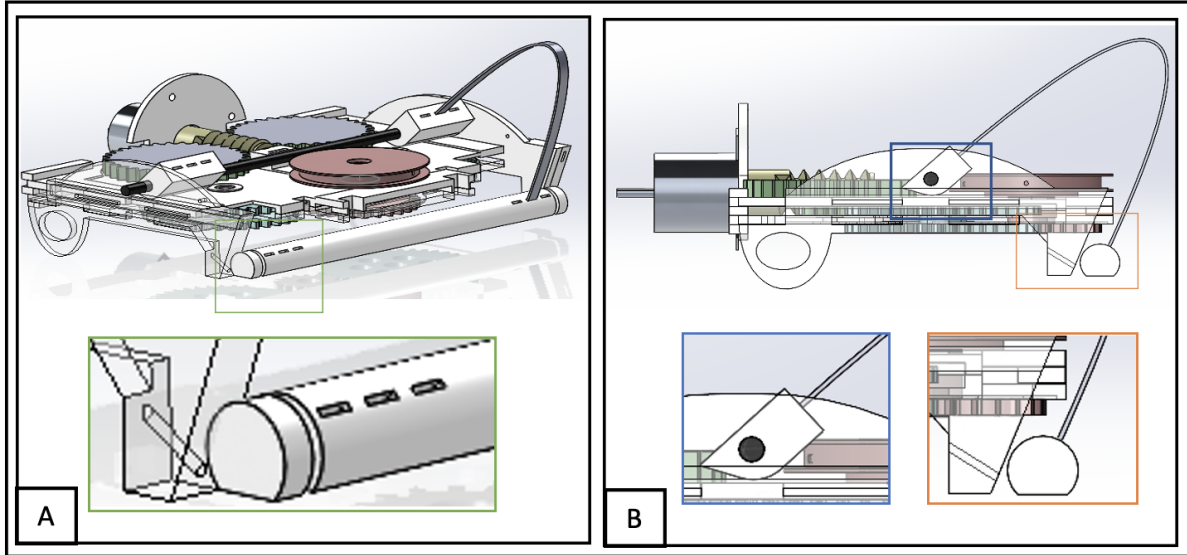


Figure 18: This image shows the springs in a compressed configuration. The image on the left (A) shows a view from the backside. It highlights the slot where the string passes through. The image on the right (B) is the side view. It shows the pivot when the spring is compressed. It also highlights the position of the end of the beam. The flat surfaces touch the ground when the springs are compressed.

5.3.2 End of beam

To stiffen the springs, we bind all the ends of the springs together. We printed a half-cylinder with holes to insert the springs. It is a half-cylinder to have a flat surface touching the ground when the springs are compressed, as shown in Fig. 18.B. We also cover the end of the beam with silicone 186 to increase friction with the ground that prevent foot slip when the robot jump. Furthermore, we made some slits in the extremity to position the string.

5.3.3 String Path

We used a fishing string to compress the end of the springs to the desired position, as shown in Fig. 19. It is a robust and thin string. The string is used to connect the end of the springs to the retractor.

To stabilize the drone during compression, the string passes through the pivot, as shown in Fig.

19. This path is essential because it forces the end of springs to be at its good place. At this position, the force is coaxial with the pivot and the centre of mass; reducing the torque applying to the drone.

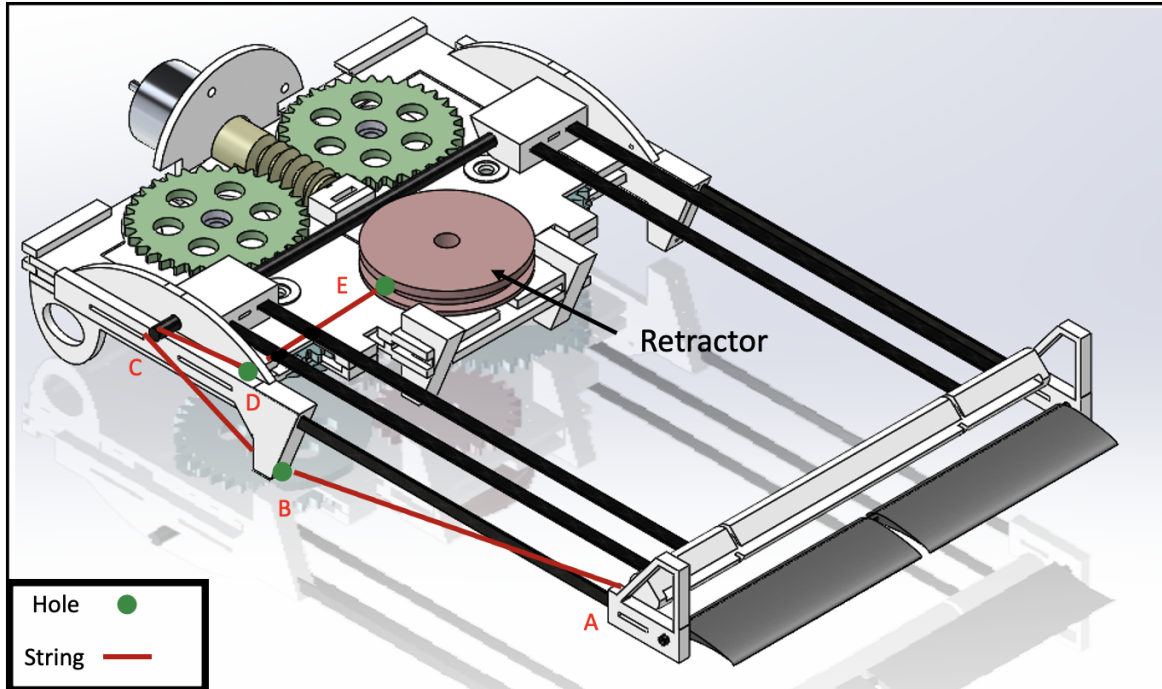


Figure 19: This image shows the path string. The string is connected to the springs in (A). After, it passes through a hole under the drone (B). Then it passes through the pivot (C) before going into another hole (D). Finally, it is connected to the retractor (E).

5.4 Wing-tail

We found that the airfoil s1223 provides high lift at a low-speed flight [17],[18] or [19]. Fig. 20 shows the lift and drag coefficients of the airfoil. It has a high lift coefficient $c_l = 2$ at 10° and a low drag coefficient $c_d = 0.03$ at 10° .

We then designed the airfoil with the help of the Aerotool website [20]. The wing has a wing length of 400mm and a wing chord of 100mm that produce a lift force of 1.5N at 6 m/s (see section 4.1 for our calculation)

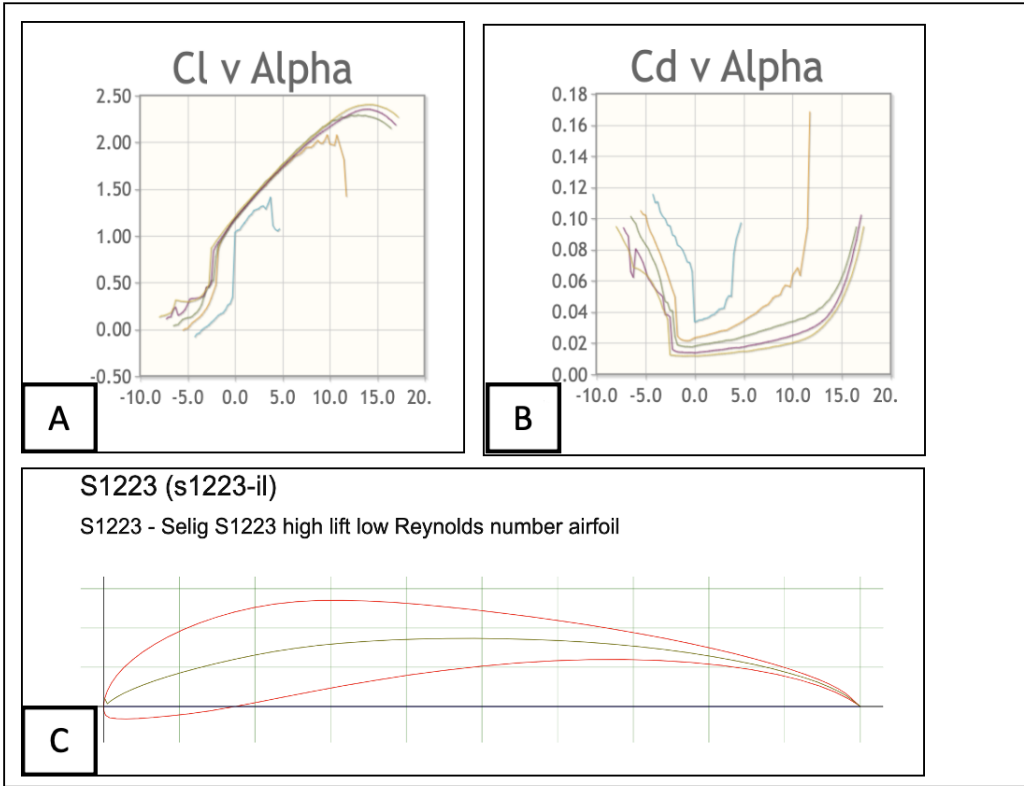


Figure 20: This image shows information of the airfoil s1223 from Aerotoll website. The first image on the top left (A) shows the lift coefficient in the function of the angle. The image in top right (B) shows the the drag coefficient in function of the angle. The image on the bottom (C) shows the airfoil profile.

The tail has three goals [21]. First, it creates some lift. Then, it counterbalances the moment of force from the wing. Moreover, it controls the pitch during flight. To design the tail, we focused on stability in flight. Thus, we counterbalanced the moment of force from the wing. We used the equation (14) to find the a surface of the tail equal to 0.003 m^2 .

$$\sum \text{Moment} = \text{DistWing} * F_{\text{LiftWing}} + \text{DistTail} * F_{\text{LiftTail}} = 0 \quad (14)$$

Another critical point is the rigidity of the tail during flight. The tail should not oscillates during a jump or other perturbation but should be lightweight enough. Thus, we used the same carbon fibre as for the springs but arranged in the sandwich and perpendicular configuration to offer a total rigidity on the bar tails as shown in Fig.21. Two different point of view is shown to well understand the different configuration of the beam, from the top (A), and from the side (B).

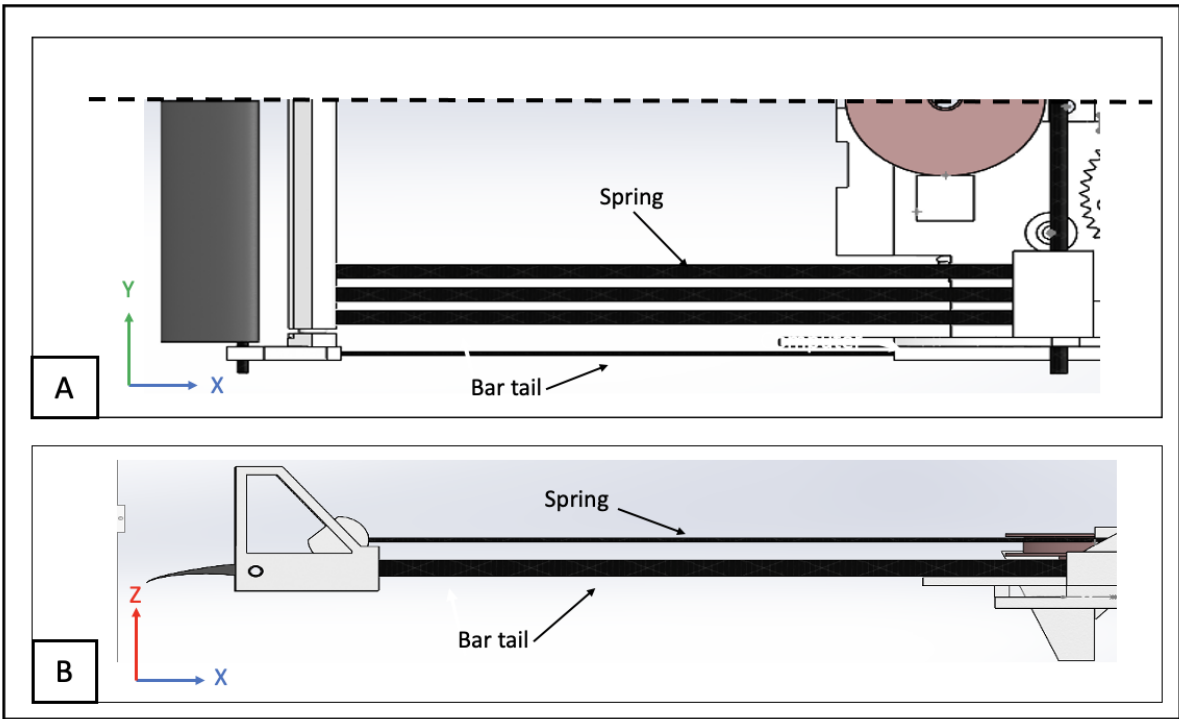


Figure 21: These images show a detail of the tail and its connection. The first image (A) shows an image from the top half-cut because of the symmetry. The image on the bottom (B) illustrates the tail from the side. These images underline that the bar tails and the springs are perpendiculars and the bar tails enrol the springs like a sandwich. That means the spring can flex in the z-direction but not in the y and x-direction. Thus, the bar tails are rigid in all directions.

5.5 Components

Table 2 lists the components used in the robot for jumping and flying experiments. We underline that we chose the components to be lightweight as possible.

Table 2: Devices

| Function | Description | Detail |
|-----------|-------------------------------------|----------------------|
| Battery | 2S lipo battery 160 MaH | Turnigy Nano-tech |
| ESC | 10A Forward, brake and reverse esc | Quik series XC-10A |
| Servos | 2 Nano servos for direction control | Scanner RC 9103MG500 |
| Motor | small brushless motor 1700kv | techno hobby AS2204 |
| Propeller | 3x3.5 inch propeller with 3 blades | 500 |
| Receiver | receiver radio | orange DRX ar4510 |

6 Prototype

To test all the concepts discussed in the previous sections, we split the experiment into parts. We first tested the spring performance to see if it gives enough speed and force for a jump, and also to validate the body rotation. Then, we tested the gearbox. The gearbox with gears and a worm gear were made of 3d printing materials. Thus, we tested if it works well and verified the behaviour of the freewheel as well. Finally, we remade the final gearbox with the decoupling mechanism incorporated. After all these tests, we built the final robot prototype.

6.1 Spring test

We built a prototype made of 3d printing material with a fishing line and carbon beams. The images are shown in Fig. 22. Inside the structure, we added some steel to increase the weight to match with the mass of the designed model. This prototype weighs 100 grams. The centre of mass is situated at the centre of rotation of the pivot, where the springs are connected. We use six springs. The operation is as follows. We compressed the springs by turning the retractor in the front. It is the cylinder in Fig. 22.A. When satisfied with the compression length, we blocked the retractor with a small piece of plastic inside the groove. Then, we disposed the prototype under a launching pad made of wood to block the end of the springs as shown in Fig. 22.D/E. We do that to test different compression lengths to avoid slipping.

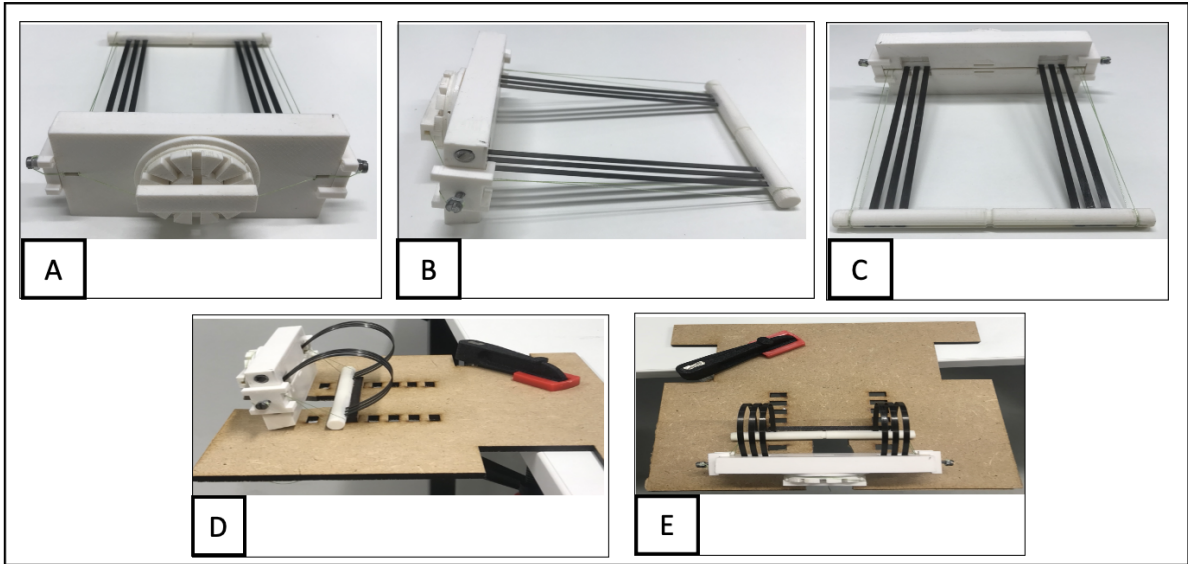


Figure 22: *This image shows the first testing prototype in two different configurations and different points of view; from the front(A), the side (B) and the back (C) in extended stage, and the side view (D) and the top view(E) when compressed in the launchpad.*

6.2 Gear box

The system is composed of one worm gear and one spur gear. We built a small structure in MDF with the laser cutter to test the gearbox. The gear needs to be custom; thus, we decided to print them in ABS with the Stratasys 3d printer. This section aims to verify the freewheel and to test different modules and gears. This step is essential because making small worm gear and spur gears in 3d printing is not easy.

Fig. 23 shows the prototype with a different view and its electronics. The worm gear can always drive the gear in both directions. But in most case the spur gears cannot drive the worm gear. We verify it with this prototype and use this specification to block the spring during compression without spend energy. However, we need now a system to release the spring when desired. It is why we design a decoupling system.

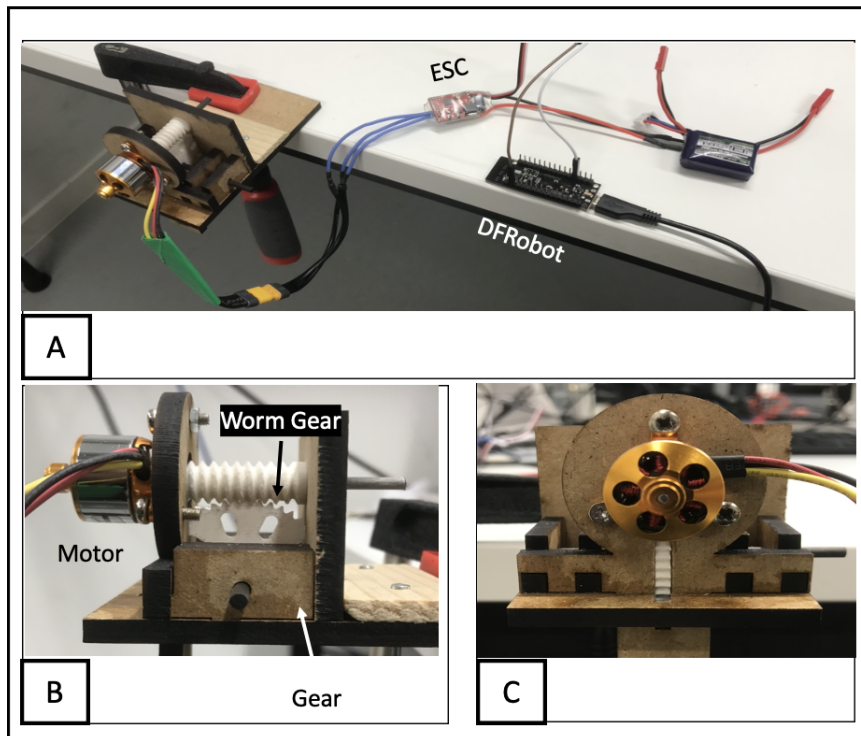


Figure 23: These images show the prototype to test the worm gear, the freewheel and the gear. The first (A) shows the mechanism with all the electronic components. We use the ESC to control the direction and the speed of the motor, the battery for the energy and the microcontroller DFRobot to control the ESC. Figure (B) is the side view and figure (C) shows the front view.

6.3 Final prototype

We built many prototypes to achieve the expected results with and without bearing, different shape of gears, number of springs, motor, shafts and so on.

Gears We spent a lot of time to design the gears and to make the gear box work well. The gears prototyping was very challenging because of the small size of the teeth and the large forces applied into them from the spring.

- We tested several gear modules between 0.5 and 1,5. The modules change the number and the size of teeth on the same diameter. That means, small module you have, bigger gain you obtain.
- We tested several materials as well. We printed the gear with the ABS and PLA materials. ABS is tougher than PLA but the precision of the ultimaker is better. Thus, when we printed in ABS the teeth was not full. That creates weak gears. You can see the details of the teeth in pla and ABS in Fig. 24.(A)
- We also tested different gear geometry. The gears we used are on layers. We first tested to print the gears separately and combined them with a carbon rod and glue (Fig. 24.(B)). However, large forces applied to the gears separated the glue. It was difficult to keep the gear in two parallel plane. Another way is that we printed the gear in one piece. But small teeth was not in the contact and gave bad results. The Fig. 24.(C) shows the final gears; made in two separate pieces in tough PLA .
- Another difficult point was the backlash between gears. Normally we need to leave a small space between them. But the 3d printer is not perfectly precise. We had to play with the size and the position of the gears to make it work.
- It was really challenging to print the worm gear with good detail and surface quality. The best way we have is to print the worm gear on Stratasys 3D printer with ABS material because of two main advantages. First, the Stratasys has a removable support by hot bath. That admits to put a lot of support around the piece to keep it precise. It is also to easily remove without damage the piece. Second, the ABS can be smoother with a vapor acetone bath. The acetone dissolve the ABS, but if you use a good timing and only the vapor, it can improve the quality of the piece and clean the state of surface [22].
- The last challenge was the friction. The friction was high and decrease the performance of the system. We added one bearing in each side to decrease the friction with the traversing axes.

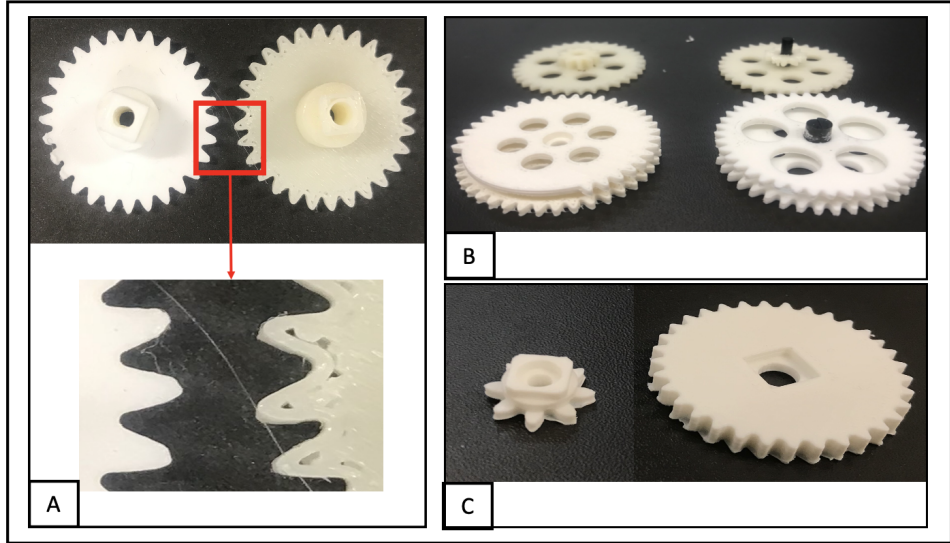


Figure 24: *Images of gears and details.* The first one (A) shows two gears with two different material (PLA on the left and ABS on the right). The red square shows a zoom of the teeth to underline that the abs has a printing less precise than pla. The second image (B) shows the different configuration to assemble gears together. The last one (C) shows the final gears in two different part to improve precision.

Decoupling mechanism This is the last part of the compressive system. We design a system that compresses the spring and releases it when it is at its optimum position. Then, it can be recompressed again and released. The Fig. 25 shows the first prototype that can compress and release the springs. It confirms that the size of the gear and all the system is working well.

Prototype ready to fly Fig. 26 shows the final prototype for flight experiments. Its weight without the wing is 160 gram. The normal wing weighs 10 gram and the larger wing weighs 20 gram. It is heavier than we expected. However, we reinforced some parts to make sure that the robot can be used for multiple tests without damage.

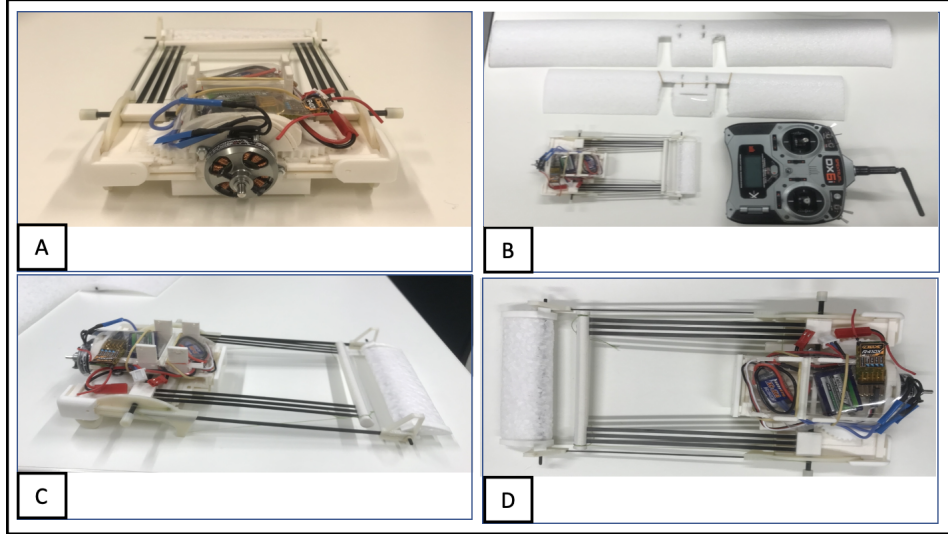


Figure 25: *Images of the final prototype in different point of view. The first one (A) is from the front. The second image (B) shows the prototype from the top with two different side of wing and the transmitter, The third image (C) is showing the prototype from the side. The last one (D) shows a view from the top.*

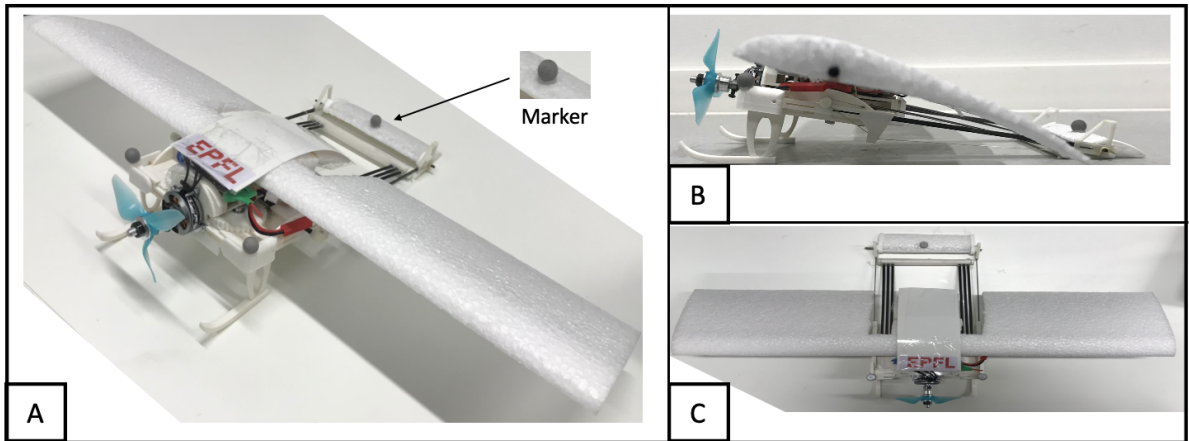


Figure 26: *Images of the final prototype ready to fly in different point of view. (A) Isometric view with a detail on the markers used to track the drone. (B) Side view and (C) top view.*

7 Experimental test

We first tested the jumps without a propeller. We characterized the jump under different configurations. We tested three different angles [35,45,55] and three different compositions [No wing, normal wing, big wing]. The normal wing is the wing designed in the simulation. We build a wing 1.8 times bigger in surface area to test the behaviour. Table (15) illustrates the plan of the experiments. We tracked the jumping performance using the OptiTrack, which is

composed of 26 cameras. We put three markers on the drone that you can see on Fig. 26. After analyzing the first test data, we tested with a propeller.

| Launching angle | No wing | Normal wing | Big wing | |
|-----------------|---------|-------------|----------|------|
| 35° | 3X | 3X | — | (15) |
| 45° | 3X | 3X | — | |
| 55° | 3X | 3X | 3X | |

8 Results

8.1 Test 1 : without propeller

This test aims to determine the effect of the launching angle and the size of the wing. With these results, we updated the prototype for experiments with the propeller.

Comparison between wings We tested three different wing configurations; No wing, normal wing, and big wing. The plot of the height and speed is on Fig. 27.A. We can see that the height and tangential speed increase from no wing to normal wing. But the performance decreases when the wing is too bigger.

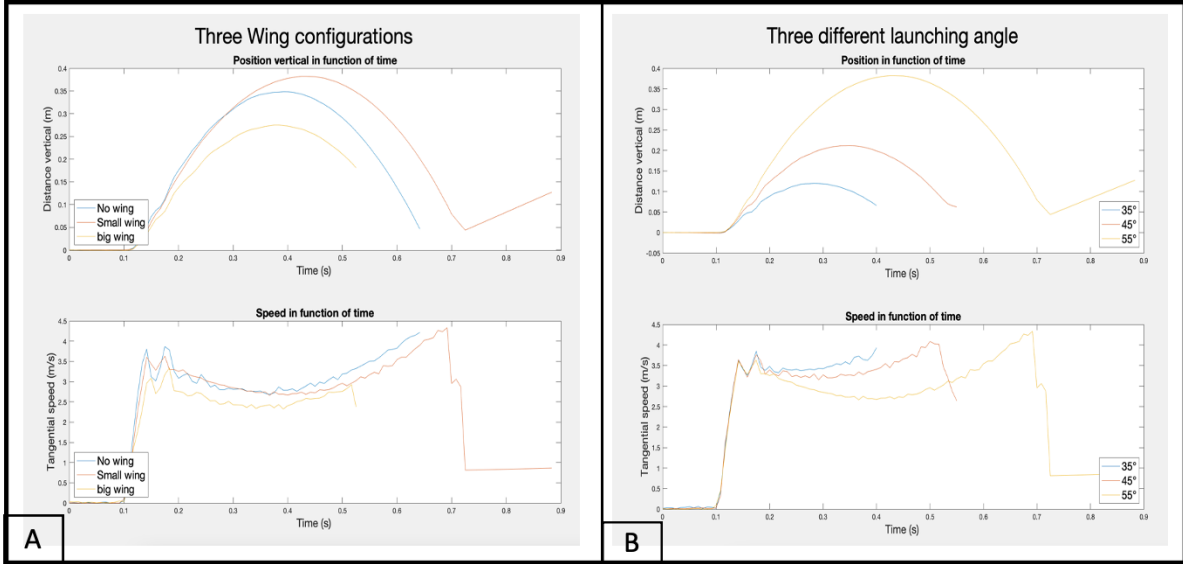


Figure 27: These are plots of the position and tangential speed on different configurations. On the top, we can see the height in the function of time. On the bottom, the tangential speed is in function of time. The plot on the left (A) has three different wing configurations; no wing, normal wing and big wing. The plot on the right (B) has three different launching angles. The normal wing offers the best performance, and the 55° angle offers excellent performance with a longer time in the air.

Comparison between launching angle We tested three launching angles; 35° , 45° and 55° . The plot of the position and speed are in Fig. 27.B. The three jumps are attractive because of their high speed (around 3.5 m/s). We remark that a more significant angle offers more height, distance, and cruising time without decreasing the velocity.

Details of the data The plots in Fig. 28 show height, distance, tangential speed and pitch angle versus time for three initial launching angles; 35° (A), 45° (B) and 55° (C). The data show a maximum tangential speed of more than 3.5 m/s. The trajectory has maximum height at 0.4 m for 55° with a distance of about 1.7 m. The most satisfying result is the pitch angle that follows the trajectory. That means the jump is controlled and has no undesirable body rotation.

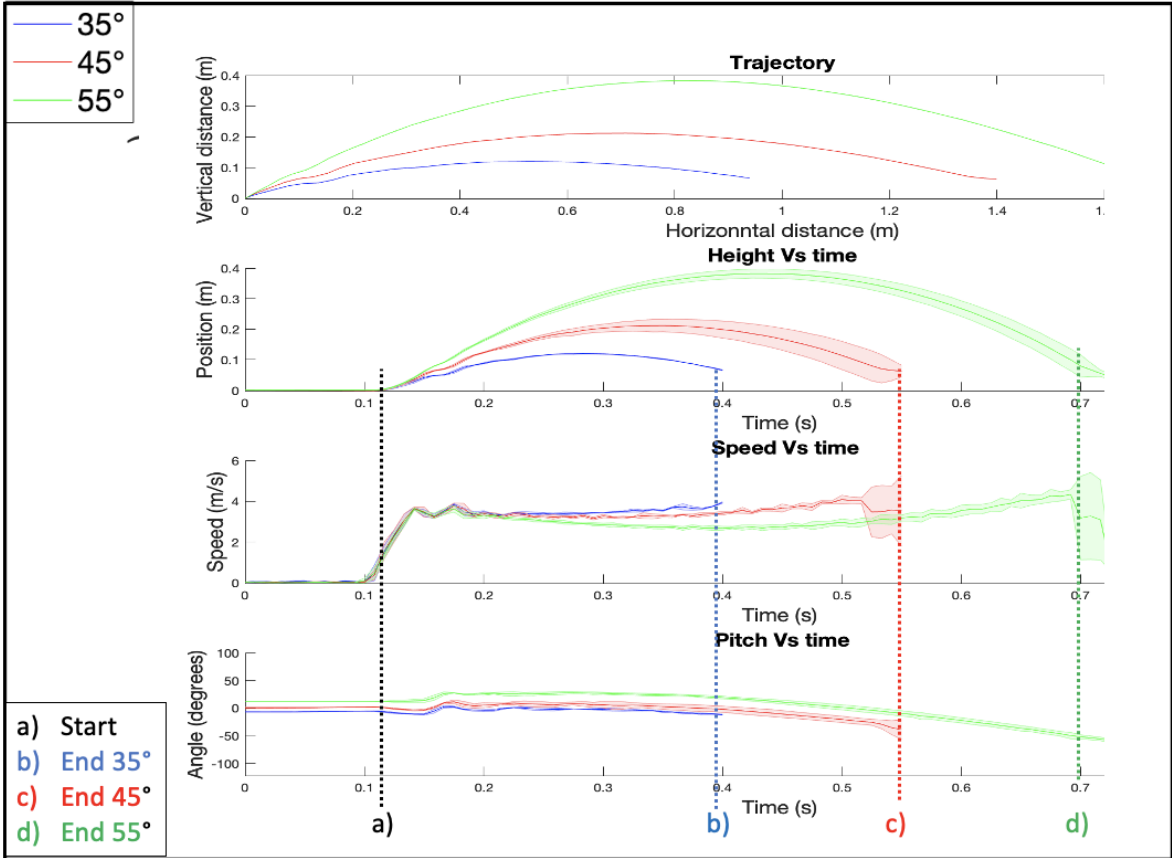


Figure 28: These are plots of different characteristics depending on the launching angle with the normal wing. The graphs from the top to bottom show the jumping trajectory, and the height, tangential speed and pitch angle versus time. The blue, red, and green lines represent for the takeoff angles of 35° , 45° and 55° , respectively. We underline the start and the end of each jump for the sake of clarity. The case of 55° offers an excellent performance (3.5 m/s, 0.4 m high and about 1.7 m long) with a longer time in the air (0.7 sec).

Discussion test 1 From the results, we can see that the robot with the normal wing launching at an angle of 55° show better performance. The big wing however decreases the maximum speed,

distance and height as shown in Fig. 27.A. In addition, the larger wing adds extra weight (10 grams heavier), and creates more drag relatively to the lift improvement.

Launching at 55° also allows the robot to reach an initial speed of more than 3.5 m/s and stay longer in the air (about 0.7 s) to activate the propeller for flying. The time in cruising is essential for us because it is when the propeller can have an effect to make it fly. Fig. 29 show the robot during the jumping experiment with an takeoff angle of 55° .

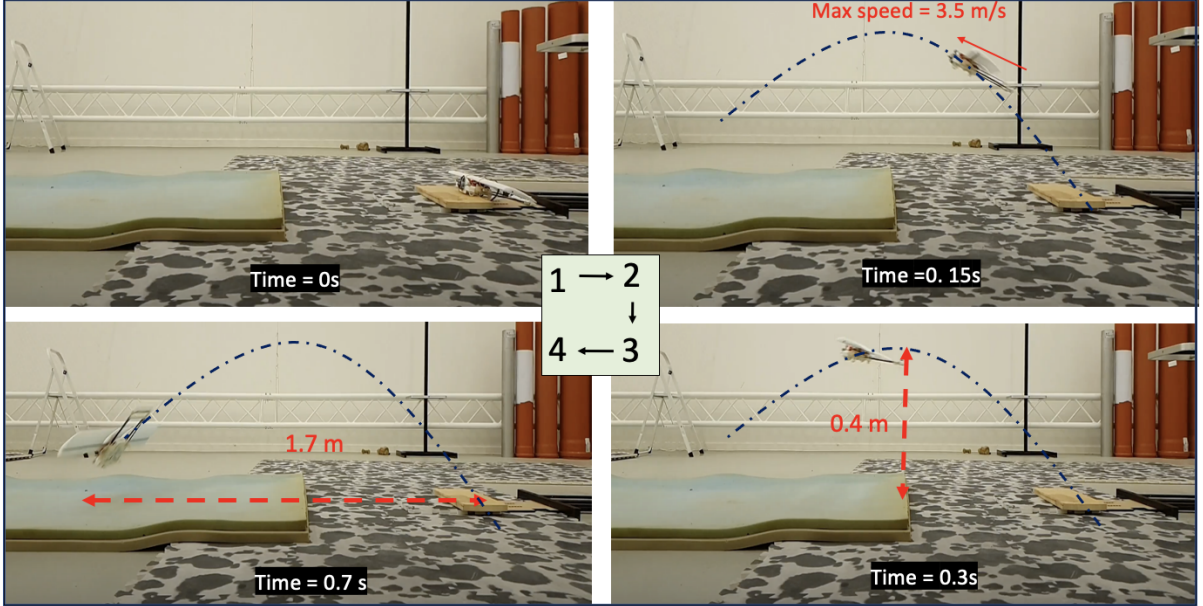


Figure 29: This set of images shows the drone’s trajectory when jumping at 55° with normal wing. The chronological order of the images is in clockwise. The maximum tangential speed is about 3.5 m/s.

8.2 Test 2 : with propeller

Unfortunately, we did not have enough time to perform this experiment for the report. However, we will do our best to show them in the final presentation.

9 Discussion

In this project, we designed a jumping-assisted takeoff mechanism for a fixed-wing drone. The system performs two different functionalities, storing elastic energy for jump and generating thrust, using a single electric motor with a change in motor rotation direction by reusing at most the structure of the typical drone. Furthermore, the high initial speed allows the robot to achieve the lift needed for flight. Most importantly, no body rotation occurs after the jumping; the jump is stable. Even if the drone can achieve the transition between jump and flight, further improvements need to be made.

The simulation for a jumping drone with the purpose to fly is complex. Because the equation that describes the physics are depending on a multitude of parameters, the mechanical design optimization for an optimal jump is complicated. The results of the simulations are different from those of the first experiment. Indeed, the investigation gives better characteristics than the simulation. This difference is undoubtedly due to the simplification of the complex bending springs into two rigid bars with a torsional spring, and also because we do not make the pivot between the springs and the body. Therefore, the model needs to be closer to reality to improve the simulation. Furthermore, the difference between simulation and experiment may come from errors in estimating the total energy inside the spring and the torque required to compress one spring.

The prototyping was also challenging due to the large force required to bend the carbon plates. In addition, the prototype needs to be as small as possible to save weight. That means small motors, small gears, and small structures. However, to make it work and resistant enough for the testing, we made the drone too heavy. Now that the concept is proven, the drone will have to be lightweight to increase its performance.

The foot of the drone has not enough friction with the floor. The high speed and the small weight of the drone make the feet slip under some circumstances when jumping. To counterbalance this problem, the geometry of the foot will have to be modified to increase the contact surface. Furthermore, the silicone around the feet will have to be tested under different floors. If these improvements are insufficient, hooks on the feet to catch the floor when takeoff could be added.

Finally, even if the trajectory and the maximum speed is promising, the time in the air is relatively short (less than 1 sec). This short time interval is not a problem for an autopilot to quickly switch from one direction of rotation to the other. However, for a human, the time of reaction is longer. Moreover, the ESC is not the most appropriate for fast switching. Thus, we could implement a code that compresses and directly active thrust to fly to counterbalance this problem. The other possibility is to increase the number of springs and the launching angle. Thus, the time in the air will be improved, and the user will have more time to add thrust. For this, the ESC will need to be configurated to let the passage between the two direction quickly.

10 Conclusion

The actual state of the art on this domain is restricted to a drone that jumps and glide, like the jumpglider of Alexis Lussier [5] and [6], or the jump glider from EPFL [7] or finally, the locust wing morphing from Avishai Beck et al [15]. Our contribution is to go on step further by offering a design that can sequentially jump and fly using components already present on the typically fixed-wing. This report exposes the primary key to simulating and designing a drone that can perform a self-landing and self-takeoff in confined spaces and keep the advantages of a fixed-wing.

The simulation part shows the primary step to describe the behaviours of the jumping drone. Firstly, it shows the power of the flow simulation from Solidworks that give us all the characteristic of a wing and its airfoil. Secondly, it explains the bending beam's behaviours used as a spring. It permits to test of different shapes, lengths, materials, curvature, and fixation to the drone (pivot). In addition, the simulation give the energy stored, the breaking point and the needed torque to compress. Finally, it characterizes the trajectory, the speed, and the body rotation in function of the spring characteristics (rigidity, initial position) and the wing and tail geometry (size, aerodynamical constraint and distance from centre mass).

The report exposes all the steps and prototypes before the final drone. All the design process is explained, and it reveals every subpart in detail to understand the advantages of this ingenious system. Thus, this report allows the reconstruction of the drone.

The experimental result recorded using the OptiTrack gives a precise and general idea of the drone's performance and the point to improve. It has shown that the drone has an excellent fluent trajectory and almost acquire the take-off speed during jumping. The drone's body nicely follows the course and permits maximizing the wing's effect to create lift. To expand on these promising results and fully explore the drone's performance, additional tests with the propeller should be performed in the future.

11 Acknowledgments

Firstly, I am grateful to the LIS laboratory for allowing me to do this project and access all the needed material and workshop. I also want, of course, to thank my supervisors for their time, help, and all the advices during the entire project. Furthermore, a particular thank you to my family and loved ones to support me during this stressful time. Finally, to my sister Tess Bonato to try at most the possibility to improve the report's writing.

References

- [1] V. Zaitsev et al. “Locust-Inspired Miniature Jumping Robot”. In: *International Conference on Intelligent Robots and Systems* (2015).
- [2] Ryuma Niiyama et al. *Mowgli: A Bipedal Jumping and Landing Robot with an Artificial Musculoskeletal System*. 2017.
- [3] Guan-Horng Liu et al. *A Bio-Inspired Hopping Kangaroo Robot with an Active Tail*. 2014.
- [4] Xiaojuan Mo et al. “Jumping Locomotion Strategies: From Animals to Bioinspired Robots”. In: *Applied Science* (2020).
- [5] Alexis Lussier Desbiens et al. “Efficient Jumpgliding: Theory and Design Considerations”. In: *IEEE ICRA* (2013).
- [6] Alexis Lussier Desbiens et al. “Design principles for efficient, repeated jumpgliding”. In: *IEEE ICRA* (2014).
- [7] Mirko Kovac et al. “The EPFL jumpglider: A hybrid jumping and gliding robot with rigid or folding wings”. In: *IEEE* (2011).
- [8] Passerine Aircraft Corporation. *Delivery Drones Use Bird-Inspired Legs to Jump Into the Air*. Newspaper. MOBOTS, EPFL, 2019.
- [9] wang-Pil Jung et al. “JumpRoACH: A Trajectory-Adjustable Integrated Jumping–Crawling Robot”. In: *TRANSACTIONS ON MECHATRONICS* (2019).
- [10] Gwang-Pil Jung et al. “An Integrated Jumping-Crawling Robot using Height-Adjustable Jumping Module”. In: *International Conference on Robotics and Automation (ICRA)* (2016).
- [11] Duncan W. Haldane et al. “Robotic vertical jumping agility via series-elastic power modulation”. In: *SCIENCE ROBOTICS* (2016).
- [12] et al. Takashi Tsuda. “A Compact Kick-and-Bounce Mobile Robot powered by Unidirectional Impulse Force Generators”. In: *IEEE/RSJ International Conference on Intelligent Robots and Systems* (2009).
- [13] et al. Mirko Kovac. “A miniature 7g jumping robot”. In: *IEEE International Conference on Robotics and Automation* (2008).
- [14] Matthew A. et al. “MultiMo-Bat: A biologically inspired integrated jumping–gliding robot”. In: *SAGE* (2014).
- [15] Avishai Beck et al. “Jump stabilization and landing control by wing-spreading of a locust-inspired jumper”. In: *Bioinspir* (2017).
- [16] Gabriel Staples. “Propeller Static Dynamic Thrust Calculation”. In: <https://www.electricrcaircraftguy.com/static-dynamic-thrust-equation-background.html> (2017).

- [17] Michael S. Selig et al. “High-Lift Low Reynolds Number Airfoil Design”. In: *JOURNAL OF AIRCRAFT* (1997).
- [18] Michael S. Selig et al. *Summary of Low-Speed Airfoil Data*. 1997.
- [19] Sumit Sharma. *An Aerodynamic Comparative Analysis of Airfoils for Low-Speed Aircrafts*. 2016.
- [20] Airfoil team et al. “Airfoil Tools”. In: <http://www.airfoiltools.com/airfoil/details?airfoil=s1223-il> (2022).
- [21] aerottolbox team. *Horizontal and vertical tail design*. <https://aerotoolbox.com/design-aircraft-tail/>. 2019.
- [22] Harry Gao et al. “Investigating the Impact of Acetone Vapor Smoothing on the Strength and Elongation of Printed ABS Parts”. In: *JOM 69* (2017).